NASA TECHNICAL NOTE

NASA TN D-8348

NASA IN D-8348

OPTIMAL ONE-SECTION AND TWO-SECTION CIRCULAR SOUND-ABSORBING DUCT LINERS FOR PLANE-WAVE AND MONOPOLE SOURCES WITHOUT FLOW

Harold C. Lester and Joe W. Posey

Langley Research Center
Hampton, Va. 23665

NATIONAL AERONAUTICS AND SPACE ADMINISTRATION • WASHINGTON, D. C. • DECEMBER 1976

1. Report No.	2. Government Accession No.	3. Recipient's Catalog No.
NASA TN D-8348		

4. Title and Subtitle	5. Report Date
OPTIMAL ONE-SECTION AND TWO-SECTION CIRCULAR SOUND-ABSORBING DUCT LINERS FOR PLANE-WAVE AND MONOPOLE SOURCES WITHOUT FLOW	December 1976
	6. Performing Organization Code

7. Author(s)	8. Performing Organization Report No.
Harold C. Lester and Joe W. Posey	L-11039
	10. Work Unit No.
	505-03-11-04

9. Performing Organization Name and Address	11. Contract or Grant No.
NASA Langley Research Center Hampton, VA 23665	
	13. Type of Report and Period Covered
12. Sponsoring Agency Name and Address	Technical Note
National Aeronautics and Space Administration Washington, DC 20546	14. Sponsoring Agency Code

15. Supplementary Notes

16. Abstract

A discrete frequency study is made of the influence of source characteristics on the optimal properties of acoustically lined uniform and two-section ducts. Two simplified sources, a plane wave and a monopole, are considered in some detail and over a greater frequency range than has been previously studied. Source and termination impedance effects are given limited examination. An example of a turbomachinery source and three associated source variants are also presented.

Optimal liner designs based on modal theory approach the Cremer criterion at low frequencies and the geometric acoustics limit at high frequencies. Over an intermediate frequency range, optimal two-section liners produced higher transmission losses than did the uniform configurations. Source distribution effects were found to have a significant effect on optimal liner design, but source and termination impedance effects appear to be relatively unimportant.

17. Key Words (Suggested by Author(s))	18. Distribution Statement
Duct acoustics Duct liners Duct liner optimization	Unclassified - Unlimited Subject Category 71

19. Security Classif. (of this report)	20. Security Classif. (of this page)	21. No. of Pages	22. Price*
Unclassified	Unclassified	51	$4.25

* For sale by the National Technical Information Service, Springfield, Virginia 22161

OPTIMAL ONE-SECTION AND TWO-SECTION CIRCULAR SOUND-ABSORBING DUCT LINERS FOR PLANE-WAVE AND MONOPOLE SOURCES WITHOUT FLOW

Harold C. Lester and Joe W. Posey
Langley Research Center

SUMMARY

A discrete frequency study is made of the influence of source characteristics on the optimal properties of acoustically lined uniform and two-section ducts. Two simplified sources, a plane wave and a monopole, are considered in some detail and over a greater frequency range than has been previously studied. Source and termination impedance effects are given limited examination. An example of a turbomachinery source and three associated source variants are also presented.

Optimal liner designs based on modal theory approach the Cremer criterion at low frequencies and the geometric acoustics limit at high frequencies. Over an intermediate frequency range, optimal two-section liners produced higher transmission losses than did the uniform configurations. Source distribution effects were found to have a significant effect on optimal liner design, but source and termination impedance effects appear to be relatively unimportant.

INTRODUCTION

In recent years much research effort has been directed toward developing mathematical models for understanding the propagation and attenuation of sound in aircraft engine ducts. In the present study, optimal one-section and two-section circular sound-absorbing duct liners are determined for plane wave and monopole sources without flow. The optimization is performed numerically by the application of an extremum algorithm to an analytical duct propagation model.

An optimal liner is achieved by judiciously selecting the impedance characteristics of the liner so that maximum sound attenuation is produced for a given design condition. The often-cited work of Cremer (ref. 1) is the earliest attempt to define an optimal liner. Cremer's approach is based on maximizing the attenuation rate of the lowest order (least attenuated) acoustical mode propagating in an infinitely long, two-dimensional duct. Optimal liner impedance values have also been determined by Rice (ref. 2) for a plane-wave source in an infinitely long, uniformly lined, circular duct without flow. Rice's model is based on the superposition of a finite number of soft-wall radial duct modes. Contour maps of constant attenuation in the impedance plane were employed to determine optimal liner impedance values. Rice found that the optimum impedance was a function of frequency and length-diameter ratio of the circular duct.

Tester (ref. 3) recently generalized and extended Cremer's results for application to rectangular and circular cross sections and to arbitrary higher order modes. This extension was motivated by the consideration that the lowest order mode does not necessarily carry most of the acoustical power. Tester showed, however, that the circular-duct generalization of Cremer's optimum impedance was the limit, for a large length-diameter ratio, of Rice's optimum impedance.

Wilkinson (ref. 4) was the first to calculate optimal liner impedance values by using an automated optimization procedure. He utilized an integral-equation propagation model coupled with the method of steepest descent. His results for uniform cylindrical liners with a plane-wave source compare favorably with Rice's results (ref. 2). Wilkinson also optimized a two-section duct and found that although the impedances of the two optimized sections were noticeably different, there was less than 1-dB increase in the duct transmission loss. In contrast to Wilkinson's result, numerical studies by Lansing and Zorumski (ref. 5) showed that multisectioned (three sections) liners may give a significant improvement over uniform liners.

Quinn (ref. 6) used a finite-difference solution of the convective wave equation to study optimal liners although details of his minimization method are not mentioned. He attempted to find the number of sections (of equal length) which, when optimized with respect to impedance, would give the largest attenuation in a given total length. A small improvement was found by Quinn with two sections (agreeing with Wilkinson), large improvements in passing to three and four sections (agreeing with Lansing and Zorumski), and finally, a further small improvement with a fifth section. Quinn also used a plane-wave source to confirm Lansing and Zorumski's result (based on a point source) that three-section liners maintain their effectiveness over a broad frequency range.

Beckemeyer, Sawdy, and Patterson (refs. 7 and 8) have also investigated the properties of optimal multisectioned ducts. Their theoretical model was based on modal superposition (mode matching method). A conjugate gradient algorithm was utilized in this optimization process. Beckemeyer and Sawdy's analytical studies defined two-section ducts which showed significant improvement over a one-section configuration and contradicted the results of Wilkinson and Quinn. Beckemeyer and Sawdy (ref. 7) have also improved the understanding of the physical process which causes multisectioned ducts to have better performance. Although Lansing and Zorumski (ref. 5) speculated that a reflection process was responsible for the behavior of multisectioned ducts, Beckemeyer and Sawdy showed that there was no significant energy reflection, but rather that there is a reflection of high order modes and a transmission of sound as high order modes which are easily attenuated by the liner in the second section. Thus, the mechanism of added transmission loss in a multisectioned duct seems to be a conditioning of the sound in one section which makes it susceptible to absorption in a following section. Sawdy, Beckemeyer, and Patterson (ref. 8) utilized their multisectioned duct optimization to design duct liners which were subsequently tested in a flow duct facility. In their design studies, they found that the source has a significant influence on the predicted attenuation of a given duct design. Their experimental results confirmed that multisectioned liners, properly designed, perform better than the best possible uniform liners.

The history of multisectioned liners is remarkable in acoustics, in that the analytical studies have led experimental work.

The main purpose of this paper is to provide a detailed investigation of the influence of source characteristics on the optimal properties of uniform and two-section ducts. The duct propagation theory, upon which the present calculations are based, is that of Zorumski (ref. 9). The numerical optimization algorithm used is that of Davidon, Fletcher, and Powell (discussed in ref. 10). Two simplified sources are considered in detail: a plane-wave source and a monopole source. Results of previously published optimization studies have generally been based on the assumption of a plane-wave source or upon a source plane pressure distribution determined by the superposition of a few radial modes with arbitrarily weighted amplitudes. The present paper also extends the frequency range of previous studies. Results in the normalized frequency range $2 \leq kb \leq 20$ are compared with simple low-frequency (Cremer) and high-frequency (geometric acoustics) approximations at the respective limits of this range. The effects of source and termination impedance, not considered in previous optimization work, are given a cursory examination in the present paper through the use of some simplified source and termination models. Although no detailed study is attempted here of more sophisticated source models, one example is presented of a turbomachinery source. Optimal liners having one, two, and three sections are determined for a theoretically exact rotor-wake and stator interaction model and are compared with results for three arbitrary source variants.

SYMBOLS

A	wave amplitude
$\bar{A}$	vector of wave amplitudes
$\bar{B}$	admittance vector
b	duct radius
c	ambient speed of sound
$\bar{D}$	ascent vector (eq. (A2))
d	liner depth
$[I]$	identity matrix
$\mathrm{Im}( )$	imaginary part of ( )
IL	insertion loss
i	$= \sqrt{-1}$

J,Y	Bessel functions of first and second kind, respectively
k	scalar wave number, ω/c
L	total length of duct liner
M	uniform flow Mach number
m	circumferential wave number
N	number of lined duct sections
$P_{m\mu}$	source pressure coefficients (eq. (13))
p	acoustic pressure
$\bar{Q}$	source vector
$Q_{m\mu}$	source velocity coefficients (eq. (15))
$Re(\ )$	real part of ( )
$\bar{R}$	vector, defined in equations (A3)
r,θ,z	cylindrical coordinates
$[S]$	positive-definite matrix (see eqs. (A3))
TL	transmission loss
t	time
u	axial acoustic velocity
$[W]$	system matrix
Z	normal acoustic impedance
$Z_{m\mu\nu}$	modal termination impedance coefficients (eq. (19)); note that $Z_{m\mu\mu} = Z_{m\mu}$
α	scalar minimization parameter
β	specific liner admittance, $\xi - i\sigma$
β_s	source admittance (eq. (14))
$\delta_{\mu\nu}$	Kronecker delta function
ζ	specific liner impedance, $\theta + i \cot(kd)$ where $\zeta = 1/\beta$

θ liner resistance (also used as cylindrical coordinate)

λ radial wave number, $\sqrt{1 + 2M\Omega - (1 - M^2)\Omega^2}$

ξ liner conductance

$\Pi(z)$ acoustic energy flux at axial coordinate z

ρ ambient density

σ liner susceptance

τ, δ constrained variables for θ and d (see eqs. (9))

ϕ incidence angle

$\psi(kr)$ radial mode function

Ω complex axial wave number (propagation constant)

ω circular frequency

$\overline{\nabla\{\ \}}$ gradient of $\{\ \}$

$\{\ \}^*$ complex conjugate of $\{\ \}$

Subscripts:

c Cremer quantity

h denotes hard wall quantity

i liner section index (i = 1, 2, . . ., N)

k iteration index

m circumferential wave number

0 initial value

s source quantity

t termination quantity

μ, ν radial mode indices

Superscripts:

$\pm$ denotes quantity associated with positive (+) or negative (-) traveling wave

$[\ ]^{-1}$ matrix inverse

$[\ ]^{T}$ matrix transpose

ANALYTICAL CONSIDERATIONS

This section reviews some of the relevant analytical considerations of optimal liner design. In particular, the essential features of a duct propagation model for calculating transmission losses are summarized. Also discussed is the associated numerical algorithm for maximizing the loss function.

Definition of Optimal Liner

Consider the uniform circular duct configuration shown in figure 1. The lined section has a radius b and length L and is assumed to have admittance $\beta(\omega,z)$ which varies with z in a stepwise fashion. A periodic source, with known modal properties, is shown located to the left of the lined section ($0 \leqq z \leqq L$) and provides an influx of acoustical energy $\Pi(0)$. In practice, the superimposed source modal properties (amplitudes and phase angles) represent the complex pressure patterns generated by the rotating blades and stators of an aircraft engine at a known operating condition. A measure of the liner's effectiveness as a sound absorber is given by the transmission loss function TL

$$TL(\beta) = -10 \log_{10} \left[\frac{\Pi(L)}{\Pi(0)}\right] \tag{1}$$

where $\Pi(L)$ is the acoustical power passing the plane $z = L$. Within the context of this paper, an optimal liner is a liner configuration possessing admittance β so that the resulting transmission loss TL is a maximum.

In the following section a propagation model for calculating the transmission loss TL (eq. (1)) is reviewed. A general purpose numerical procedure is then described for maximizing the transmission loss TL with respect to the liner admittance β.

Propagation Model

For the present study, the mode summation propagation theory developed by Zorumski (ref. 9) for multisectioned, axisymmetric ducts is employed. The essential element of Zorumski's mathematical duct model is the harmonic ($e^{-i\omega t}$) solution of the convective wave equation for the mth circumferential harmonic of the complex pressure:

$$p_m^{\pm}(r,z) = \rho c^2 \sum_{\mu=1}^{\infty} A_{m\mu}^{\pm} \psi_{m\mu}^{\pm}(kr) e^{i\Omega_{m\mu}^{\pm} kz} \tag{2}$$

The pressure $\sum_{m=0}^{\infty} p_m^{\pm}(r,z)e^{i(m\theta-\omega t)}$ represents an exact solution for an infinitely long duct having uniform wall admittance properties. The $\pm$ superscripts indicate that the pressure field is composed of a superposition of left (-) and right (+) moving waves. For a given circumferential wave number m, the corresponding axial wave numbers $\Omega_{m\mu}^{\pm}$ and radial mode functions $\psi_{m\mu}^{\pm}(kr)$ are determined from the cross-sectional geometry and the wall (liner) admittance β. The mode functions $\psi_{m\mu}(kr)$ for a circular duct are Bessel functions of the first kind. Each term in the modal series (eq. (2)) is weighted by a complex coefficient $A_{m\mu}^{\pm}$ which serves as a generalized coordinate to be determined.

A multisectioned liner configuration consists of a union of several liner sections each possessing uniform admittance properties. Within each section the pressure can be expressed in series fashion as in equation (2). Of course, the parameters β, $A_{m\mu}^{\pm}$, and $\Omega_{m\mu}^{\pm}$ and the mode functions $\psi_{m\mu}^{\pm}(kr)$ vary from section to section. The coefficients $A_{m\mu}^{\pm}$ for adjacent liner sections are coupled by imposing pressure and velocity continuity conditions at the section interfaces. Zorumski shows that this approach readily leads to the definition of transmission and reflection matrices. The governing equation for the multisectioned duct liner configuration is then expressible in a matrix format as

$$[W]A = \bar{Q} \tag{3}$$

with solution

$$\bar{A} = [W]^{-1}\bar{Q} \tag{4}$$

The system matrix $[W]$ is a non-Hermitian complex matrix whose non-null off-diagonal submatrices account for the transmission and reflection effects. The elements of the source vector $\bar{Q}$ consist of the modal coefficients, generally complex, of an acoustic source located within the configuration. The elements of the vector $\bar{A}$ are the modal coefficients $A_{m\mu}^{\pm}$ of the various sections.

Of particular importance in the following will be the transmission loss TL (in decibels) as given by equation (1). In this equation $\Pi(0)$ is the input axial acoustical energy at the source plane $z = 0$ (see fig. 1) and $\Pi(L)$ is the exit energy flux from the last lined section. In lieu of transmission loss, some researchers use insertion loss IL which is obtained by replacing $\Pi(0)$ in equation (1) by the input axial acoustical energy $\Pi_h(0)$ provided by the source if it were located in an infinitely long, hard-walled duct. The axial

energy flux $\Pi(z)$ at an arbitrary section located at coordinate z is given by Cantrell and Hart (ref. 11) as

$$\Pi(z) = \frac{1}{2} \mathrm{Re}\left[\int_0^{2\pi} \int_0^b (p + \rho c M u)\left(u + \frac{M}{\rho c} p\right)^* r \, dr \, d\theta\right] \tag{5}$$

where p is the complex pressure, u is the axial acoustic particle velocity, M is Mach number, ρ is the ambient density, c is the ambient speed of sound, $( )^*$ denotes complex conjugation, and $\mathrm{Re}( )$ indicates that only the real part of the quantity in brackets contributes to the flux $\Pi(z)$.

In a following section a numerical strategy is discussed for predicting the liner admittance value which gives a maximum transmission loss TL. It is therefore convenient to define an admittance vector $\bar{B}$ for a duct with N lined sections as follows:

$$\bar{B} = \begin{Bmatrix} \xi_1 \\ -\sigma_1 \\ \xi_2 \\ -\sigma_2 \\ \cdot \\ \cdot \\ \cdot \\ \xi_N \\ -\sigma_N \end{Bmatrix} \tag{6}$$

where ξ_i and σ_i are the real (conductance) and imaginary (susceptance) parts, respectively, of the liner admittance of the ith section.

Constraint Equations

It is assumed throughout the analysis that the duct wall liner is of the single-layer locally reacting type with a specific normal acoustical impedance ζ given as follows:

$$\zeta = \theta + i \cot(kd) \tag{7}$$

The impedance properties expressed by equation (7) are typical of the cavity-backed, perforated face sheet types presently used for noise abatement in the nacelles of commercial jet aircraft. The mathematical model (eq. (7)) assumes

that the face sheet is nonreactive and has a resistance θ. The nondimensional cavity depth is denoted as kd. The reciprocal of the impedance ζ is the liner admittance β; that is,

$$\beta = \frac{1}{\zeta} \tag{8}$$

In order to constrain the liner impedance variables θ and kd to physically realizable ranges, the following transformation of variables was used:

$$\left.\begin{aligned} \theta &= 5(1 + \cos \tau) \\ kd &= \frac{\pi}{2}(1 + \cos \delta) \end{aligned}\right\} \tag{9}$$

This change of variables (eqs. (9)) assumes that

$$\left.\begin{aligned} 0 \leqq \theta \leqq 10 \\ 0 \leqq kd \leqq \pi \end{aligned}\right\} \tag{10}$$

Thus τ and δ were utilized as the free variables in the numerical optimization process.

Initial values of τ and δ, for the uniform liner configurations, were generally based on Cremer's least attenuated mode criterion (refs. 1, 3, and 12). For a circular duct liner, Cremer's optimum admittance is

$$\beta_c = \frac{2.98 - 1.28i}{kb} \tag{11a}$$

as given by Zorumski. (See eq. (4) of ref. 12.) Based on the eigenvalue for the (0,0) and (0,1) mode pair, the associated transmission loss is

$$TL_c = -8.69\,\mathrm{Im}(L\Omega_1) \tag{11b}$$

where Im( ) denotes the imaginary part, L is length, and (eq. 5(c), ref. 12)

$$\Omega_1 = \frac{1}{kb}\left[(kb)^2 - (2.98 - 1.28i)^2\right]^{1/2} \tag{11c}$$

Initial values for τ and δ can be calculated from equation (11a) with the aid of equations (7) to (9).

Source Impedance Equation

Within the framework afforded by the Zorumski propagation model (ref. 9), a number of different source models can be easily represented. Perhaps the simplest is a wave source, where the right-moving waves are specified at the source plane ($z = 0$). Reflections from impedance discontinuities, although permitted, are assumed not to alter the distributions of source mode amplitudes and phase angles. This type of source is used extensively throughout the present paper.

In reality, however, the source and duct pressure fields interact. That is, the acoustic field induces a back loading on the source mechanism which alters its capacity to generate acoustical energy. This coupling effect can be studied by defining a transfer impedance as suggested in figure 2.

Pressure source.- The coupling shown in figure 2(a) defines what is termed as a pressure source. Here Z_s, which is a complex frequency-dependent variable, represents the transfer impedance between the source and duct. The transfer impedance Z_s is also a function of position on the source plane; however, this dependence is ignored to simplify the present problem. The acoustic pressure to the left of the source plane ($z = 0$) is the source pressure p_s, which is expressed in terms of its modal characteristics. (See eq. (2).) The acoustic particle velocity distribution at the source plane is denoted as u. Therefore, the acoustic pressure p to the right of the source plane is given by

$$p = p_s - Z_s u \tag{12}$$

where Z_s is the source impedance. In the absence of flow, the duct modes are orthogonal so that each right-moving mode is coupled only to its left-moving counterpart at the source plane. (See ref. 9.) Hence, each such mode pair must satisfy the source impedance condition (eq. (12)) independently of the other mode pairs. By using equations (2) and (12), there follows

$$A^+_{m\mu} = \left(\frac{1 - \Omega_{m\mu} Z_s}{1 + \Omega_{m\mu} Z_s}\right) A^-_{m\mu} + \frac{P_{m\mu}}{1 + \Omega_{m\mu} Z_s} \tag{13}$$

in which $P_{m\mu}$ denotes the modal coefficients of the source pressure distribution. Here m is the circumferential wave number and μ is the radial mode index. Equation (13) is a special case of the general form suggested in reference 9 for the representation of the source.

Velocity source.- Equivalently, a velocity source can be defined (ref. 13) as shown in figure 2(b). The source "particle" velocity u_s is specified at the source plane $z = 0$. The acoustic pressure to the right of the source plane is denoted by p. The particle velocity u is then given by the following equation:

$$u = u_s - \beta_s p \tag{14}$$

where $\beta_s = Z_s^{-1}$ is the source admittance. The relationship between the modal amplitudes is then

$$A_{m\mu}^{+} = \frac{\beta_s - \Omega_{m\mu}}{\beta_s + \Omega_{m\mu}} A_{m\mu}^{-} + \frac{Q_{m\mu}}{\beta_s + \Omega_{m\mu}} \tag{15}$$

where $Q_{m\mu}$ denotes the modal coefficients of the source velocity distribution.

Plane-wave source.- A plane-wave source, as defined in this paper, is a source such that the superposition of positive traveling waves at the source plane $z = 0$ gives a uniform acoustic pressure distribution. The effect of negative traveling waves on the source pressure distribution is neglected. Details by which the plane-wave modal coefficients $P_{m\mu}$ (eq. (13)) can be derived are given by Rice (ref. 2) and are as follows:

$$A_{0\mu} = \frac{\sqrt{2}\, J_1(\lambda_\mu kb)}{\sqrt{\lambda_\mu^2 - \beta^2}\, J_0(\lambda_\mu kb)} \tag{16}$$

where β is the source-plane liner admittance value and the λ_μ values are the solutions of

$$\left[\frac{dJ_0(\lambda_\mu kr)}{dr} - ik\beta J_0(\lambda_\mu kr)\right]_{r=b} = 0 \tag{17}$$

Monopole source.- The modal coefficients $Q_{0\mu}$ (eq. (15)) for a monopole source at $r = 0$ and $z = 0$ may be derived from the generalized results given by Zorumski. (See discussion pertinent to eqs. (19) and (38) of ref. 9.) The expressions for the source admittance β_s and the $Q_{0\mu}$ values are as follows:

$$\beta_s = \Omega_{0\mu} = \Omega_\mu \tag{18a}$$

$$Q_{0\mu} = \frac{-i\pi\lambda_\mu Q \ \Delta b\left[Y_0(\lambda_\mu kr)\right]}{\frac{\partial}{\partial\lambda_\mu}\left\{\Delta b\left[J_0(\lambda_\mu kr)\right]\right\}} \tag{18b}$$

$$\Delta r\left[Y_0(\lambda_\mu kr)\right] = \frac{dY_0(\lambda_\mu kr)}{dr} - ik\beta Y_0(\lambda_\mu kr) \tag{18c}$$

$$\Delta r\left[J_0(\lambda_\mu kr)\right] = \frac{dJ_0(\lambda_\mu kr)}{dr} - ik\beta J_0(\lambda_\mu kr) \tag{18d}$$

Termination Impedance

In general, when sound propagating through a duct reaches a termination, a radiated wave and a reflected wave are produced. For the zero flow case, the relationship between modal pressures and velocities may be expressed in terms of a modal impedance $Z_{m\mu\nu}$ (ref. 13) as follows:

$$p_{m\mu} = \sum_{\nu=1}^{\infty} Z_{m\mu\nu} u_{m\nu} \tag{19}$$

In order to simplify the present study, let the actual modal impedance $Z_{m\mu\nu}$ be represented by the direct termination impedance $\delta_{\mu\nu}Z_{m\mu\mu}$ and designate these impedances as $Z_{m\mu}$. In terms of the modal amplitudes at the termination plane $z = L$, the impedance condition is given by

$$A^-_{m\mu} = \frac{1 - \Omega_{m\mu}Z_{m\mu}}{1 + \Omega_{m\mu}Z_{m\mu}} A^+_{m\mu} \tag{20}$$

Optimization Method

An optimal liner configuration is one whose admittance properties, as expressed through the admittance vector $\bar{B}$, produce a maximum transmission loss TL. A number of researchers (refs. 4 and 6 to 8) have recently considered numerical optimization algorithms in conjunction with mathematical models of multisectioned duct liners. The authors of this paper initiated a similar research effort by combining Zorumski's (ref. 9) multisectioned duct theory and the optimization algorithm of Davidon, Fletcher, and Powell (DFP method, ref. 10).

The Davidon-Fletcher-Powell (DFP) optimization method is representative of a general class of numerical algorithms known as descent (or ascent) methods. Herein, this method is referred to as an ascent method since the duct optimiza-

tion problem has been defined in terms of maximizing the loss function. A brief review of the DFP method is given in the appendix. The defining feature, however, is that the solution vector $\bar{B}$ is obtained as the limit of a sequence

$$\bar{B}_{k+1} = \bar{B}_k + \alpha_k \bar{D}_k \qquad (k = 0, 1, 2, \ldots) \qquad (21)$$

where α_k is a scalar parameter, $\bar{D}_k$ is an ascent vector, and k is the iteration index. The iterative process begins by assuming an initial value $\bar{B}_0$ for the admittance vector. The rationale for defining the ascent vector $\bar{D}_k$ and determining the parameter α_k is discussed in the appendix. The new or modified admittance vector $\bar{B}_{k+1}$ for each iteration step is chosen so that the transmission loss TL increases in value. The iteration sequence is continued until convergence to a maximum is achieved.

Ascent optimization algorithms, in general, will locate solutions which are local (that is, relative) maxima. Thus, if the problem has multiple local maxima, different initial values $\bar{B}_0$ may iteratively converge to different "solutions" (local maxima) in the admittance space with different transmission loss values. Also, when a maximum is located in a relatively flat region of the function space, the solution may vary because of differences in convergence criteria and direction from which the maximum is approached. Luenberger (ref. 10) gives an excellent discussion of these anomalies and the reader is referred to this reference for additional discussion.

DISCUSSION OF RESULTS

Optimal liner properties calculated by the Davidon-Fletcher-Powell (DFP) numerical optimization algorithm are presented. Plane-wave and monopole sources, as well as an example of a turbomachinery source, are considered. Cremer's criterion (refs. 1, 3, and 12) was used as a starting point for all uniform liner configurations. Optimal admittance values determined numerically for the uniform liners were generally used as the initial solutions for the corresponding multisectioned cases.

As defined by equation (16), a plane-wave source infers a uniform source-plane pressure distribution as approximated by the superposition of a finite number of positive traveling waves (radial modes). Generally, only five radial modes were used for this source type. However, several ten mode cases were used for higher kb values in order to validate the five mode approximation. The modal coefficients for the monopole source are defined in equation (18). All monopole source results are based on the superposition of ten radial modes.

Infinite Duct With a Uniform Liner

Optimal properties are presented in this section for an infinite uniform liner in a circular duct (fig. 3). The source is taken to be at $z = 0$ and the transmission loss TL is maximized over the interval $z = 0$ to $z = L$.

First, a plane-wave source is studied and then a monopole source, located on the duct axis, is considered.

Plane-wave source.- Optimal admittance properties and their associated maximum transmission losses are presented in figure 4 and table I for the uniform, infinite liner configuration illustrated in figure 3. Data are presented for a frequency range $2 \leqq kb \leqq 20$ and for a length-diameter ratio of unity ($L = 2b$). The solid curves in figure 4 were calculated by the DFP algorithm. Cremer's analytical approximations (eq. (11)) and Rice's graphical results (ref. 2) are also shown in figure 4 for comparison.

Although Cremer's criterion provided adequate initial estimates for admittance, there are discernible differences between the optimal admittance values predicted by these two methods, as is clearly illustrated in figures 4(b) and 4(c). The optimal conductance given by the DFP solution is as little as two-thirds of the Cremer value in the frequency range ($4 \leqq kb \leqq 6$), but approaches the Cremer value at higher frequencies. The optimal susceptance, however, is at least 2 to 3 times the Cremer value for all frequencies where $kb \geqq 4$. The associated transmission loss for Cremer's criterion (eq. 11(b)) is shown by the dashed curve in figure 4(a) and is provided only to indicate a baseline trend. Since equation (11a) is based on the exponential decay of a single mode (the least attenuated mode), it predicts unrealistically high losses of several decibels for $kb \geqq 4$. Such losses are clearly not possible since the maximum losses are given by the DFP and Rice solutions. This condition was confirmed by taking several of Cremer's optimal admittance values from figures 4(b) and 4(c) and calculating the loss by use of the Zorumski duct propagation model. Although these data are not shown, in all cases the computed transmission losses were less than the predicted optimal DFP solutions.

The optimal transmission losses obtained from Rice's paper (ref. 2) are indicated by the short-long dashed curve in figure 4(a). The associated admittance values and the DFP values are virtually indistinguishable when plotted and both are indicated by the solid curves in figures 4(b) and 4(c). Rice utilized a similar mathematical model for the propagation calculations, although optimal admittance values were evidently determined from constant attenuation plots in the admittance plane. Two such plots obtained during the course of the present study are illustrated in figure 5.

In the case of uniform liners, for which the admittance space is two-dimensional, contour plots of constant transmission loss are useful in showing the liner performance over a fairly large region in the admittance plane for a given value of the normalized frequency kb. Figure 5(a) is for $kb = 2.0$ and illustrates that more than one relative maximum of the transmission loss may exist. Here there are two relative maxima of essentially the same magnitude (transmission loss) which occur for different admittance values. Starting the DFP algorithm at the Cremer point (eq. (11a)) gives a solution of about 49.8 dB with $\beta = 1.55 - 1.29i$. However, starting at the indicated point ($\beta = 1.30 - 2.20i$) gives a solution of 47.6 dB at an admittance value of about $\beta = 1.68 - 2.62i$. The figure clearly indicates that with ascent algorithms, the final solution can be a function of the starting point. It should be noted that the dashed lines indicate only the general direction of convergence and not the specific direction taken by the DFP numerical procedure.

A contour plot for a normalized frequency of $kb = 3.0$ is shown in figure 5(b). Only one extremum is found in the region of interest, which seemed to be typical for all cases with $kb \geq 3.0$. Here the transmission loss peak is well defined; that is, the maximum does not occur in a relatively flat region (as was the case for $kb = 2.0$) which could cause convergence problems with the DFP algorithm. A maximum transmission loss of slightly more than 30 dB is indicated for a liner with an admittance value of about $\beta = 0.80 - 0.78i$. This result is in excellent agreement with the DFP solution (fig. 4 and table I) and Rice's solution (ref. 2).

Monopole source.- Figure 6 gives the maximum transmission losses and admittance properties of the infinite uniform liner (fig. 3), introduced in the preceding section, a monopole source being located on the duct center line at $z = 0$. Thus, the situation is axisymmetric and only duct modes with zero circumferential wave number are excited. Initial admittance values, again based on Cremer's criterion (eq. (11a)), and the corresponding DFP solutions are summarized in table II.

For low frequencies ($kb \leq 3$), when only the lowest order radial mode is cut on, the trend given by Cremer's criterion agrees fairly well with the numerically optimized solutions. However, significant differences in the two predictions occur as soon as the first higher order radial mode begins to propagate. For reference, the hard-wall cut-on conditions for the first seven $m = 0$ radial modes occur at $kb = 0.0$, 3.83, 7.02, 10.17, 13.32, 16.47, and 19.62. Cremer's criterion predicts a maximum transmission loss of less than 4 dB at a $kb = 20$, whereas a numerically optimized liner can theoretically give about 10-dB loss. This is simply because higher order radial modes are much more strongly excited by a monopole source at higher frequencies. The oscillatory character of the optimal admittance, as displayed in figures 6(b) and 6(c), can probably be attributed to the multimodal nature of this particular type of acoustic source.

Since one generally has difficulty in forming a clear mental picture of acoustical propagation expressed as the sum of many modes, it is of value to compare the high-frequency behavior of the numerically optimized liner of figure 6 with the predictions of geometrical acoustics. When $kb \gg 1$, geometrical acoustics is applicable for a monopole source in a short duct and a ray-tracing solution is a valid approximation. Therefore, the acoustic pressure and particle velocity at any point on the duct section at $z = L$ may be found by summing the contributions from the direct ray and all the reflected rays passing through that point. (See fig. 7.) From this viewpoint, the best that any liner could do would be to completely absorb all incident rays, and thereby reduce the acoustic wave at $z = L$ to only the direct radiation. For $L = 2b$, only 11 percent of the rays emitted from the right side of the source are radiated directly through the $z = L$ cross section; thus, an upper limit for the transmission loss of 9.6 dB ($kb \gg 1$) is implied. Figure 6(a) shows that the optimal transmission loss predicted from the modal theory settles down to about this value as kb approaches 20.

Naturally, no uniform point-reacting liner could provide complete absorption of all incident rays, since the angle of incidence ϕ and the distance from the course $b/\cos\phi$ are not constant. Complete absorption occurs only

when the surface admittance in the direction of the incident ray is equal to the specific acoustic admittance of a spherical wave at the appropriate distance from the source. When normalized with respect to the characteristic admittance of the medium, this specific admittance is $1.0 + i\frac{\cos\phi}{kb}$. Because the rays are not normal to the locally reacting liner, the required normal admittance is not this spherical wave admittance, but is this quantity multiplied by $\cos\phi$. (See ref. 14.)

In estimating the optimal uniform liner admittance from geometrical acoustics considerations, it is reasonable to assume that any ray at $z = L$ which has been reflected off the liner more than once makes a negligible contribution to the acoustic disturbance. Figure 7 shows a ray which is reflected only once and then just clears the end of the duct. Such a ray strikes the liner at $z = L/3$ and any ray which hits the duct wall closer to the source will suffer multiple reflections. Therefore, using a single reflection criterion requires maximizing absorption for rays which first contact the liner between $z = L/3$ and $z = L$. For such rays, the average value of $\cos\phi$ is approximately 0.7, and implies an optimal normal admittance of about $0.7 + \frac{0.5i}{kb}$. The real and imaginary parts of the optimal admittance are in good agreement with geometrical predictions for large kb (figs. 6(b) and 6(c)).

Geometrical acoustics cannot be used to estimate the optimal admittance and attenuation for a plane-wave source, because in that case, all rays are directed parallel to the duct axis and suffer no reflections.

Source and Termination Impedance Effects on Optimal Liner Configurations

In this section the effect on optimal liner performance of source and termination impedance conditions is briefly examined. In previous sections, results for various types of wave sources have been presented; that is, the source modal properties were defined solely in terms of the amplitudes and phase angles of the positive traveling waves (modes) at the source plane. Alternatively, the noise source can be coupled to the duct by specifying a source impedance. (See discussion pertinent to eqs. (12) and (14).) Hence, either the source pressure or velocity contribution along with the source impedance can be specified. In a similar manner a termination impedance can be defined. (See eq. (19).) The results presented in the preceding sections were based on a traveling wave system, no left moving modes being allowed in accordance with the infinite uniform duct assumption. However, many researchers (see ref. 6, for example) use an impedance condition, usually $Z_t = 1$ (that is, a ρc termination), at the duct exit plane.

Results presented in this section are for a finite uniform liner configuration. However, the optimization algorithm was initialized at the optimal admittance values for the corresponding liner of infinite length.

(See fig. 3 and table I.) Also, since the energy radiated from the source is a function of Z_s and the liner properties, the optimal liner is defined in this section to be the one which produces the maximum insertion loss.

Source impedance.- In table III the maximum insertion losses for a one-section liner are tabulated for several values of the normalized frequency kb. Three different source types are considered: (1) a plane-wave source as used in the preceding sections, (2) a uniform pressure source with zero impedance ($Z_s = 0$, eq. (13)), and (3) a uniform velocity source with zero admittance ($\beta_s = 0$, eq. (14)). In all three cases a radiation condition was imposed at the hard-wall exit plane. (There are no negative moving waves in the region $z > L$; see fig. 1.) For $kb = 14$ and above, the maximum insertion loss varies by not more than 0.2 dB among the different source models and the corresponding optimal liner admittances (not shown) are identical within the limits of the convergence criteria. As kb decreases, the variation grows until there is a spread of about 2 dB at $kb = 4.0$. Here the optimal liner for the pressure source has an admittance of $\beta = 0.45 - 0.61i$ and for the velocity source $\beta = 0.41 - 0.51i$. In the lower frequency range ($kb < 4$), much larger differences in maximum insertion loss occur, but the corresponding optimal admittance values are essentially the same. For example, at $kb = 2$ the admittances are $\beta = 1.47 - 1.13i$, $1.48 - 1.20i$, and $1.43 - 1.08i$ for the wave, pressure, and velocity sources, respectively. Hence, the assumed source impedance seems to have little effect on the admittance of an optimal uniform liner, although some discrepancies among corresponding insertion losses can occur, particularly at the lower frequencies.

Notice that both table I and part (a) of table III present optimal properties for a uniform liner and a plane-wave source. However, in table I the liner is infinite in length (no negative moving wave, fig. 3(a)), whereas in table III, the liner terminates in the hard wall at $z = L$, reflections from this interface being accounted for. Also, the transmission loss is maximized in table I, whereas the insertion loss is maximized in table III, although there appears to be little practical difference in these criteria for the cases studied. A comparison of the two tables shows little difference in the optimal admittances at any kb value. Nonetheless, the finite liner produces considerably more attenuation than does the same length of infinite liner for $kb < 4$, when only one hard-wall duct mode is cut on.

Termination impedance.- A similar study of the effect of the exit-plane termination condition on optimal liner performance was conducted with similar results as summarized in table IV. For example, at $kb = 1.57$, a maximum insertion loss of 53.1 dB was calculated for a uniform pressure source with a radiation condition (no reflected modes) imposed at the liner termination. On the other hand, an insertion loss of only 42 dB is calculated for this pressure source with a $Z_{m\mu} = 1$ (eq. (20)) termination impedance for all modes. Comparable data from Quinn's paper (ref. 6) are also summarized in table IV. By considering basic differences in the mathematical models (Quinn employed a finite-difference solution), the agreement is fairly good. A measurable difference in optimal liner properties for the two different types of termination was calculated only at the lowest value of kb (1.57).

Infinite Duct With an Admittance Discontinuity

Optimal properties are presented in this section for an infinite duct with a source at $z = 0$ and an admittance discontinuity at $z = L/2$ (fig. 8). The transmission loss is optimized over the interval $z = 0$ to $z = L$. This configuration is sometimes referred to herein as "two-section."

Plane-wave source.- Transmission losses for the optimal uniform (fig. 3) and two-section configurations are compared in figure 9(a). Clearly, configurations with two lined sections are superior for this plane-wave source and $kb < 10$. The knee in the attenuation curve at about $kb = 4$ is most likely associated with second-mode cut-on, which for a hard-wall section, occurs at $kb = 3.83$. Quinn (ref. 6, fig. 1) noticed a similar behavior for a configuration with three sections.

The uniform liner optimal admittance values (fig. 4 and table I) were taken as starting points for the DFP algorithm. Optimal admittance properties for two sections are plotted in figures 9(b) and 9(c) and are also summarized in table V. Note here that $\xi \approx 0$ for the first sections if $kb > 5.0$. This effect has been observed by Beckemeyer and Sawdy (ref. 7) for a two-dimensional duct liner with two sections. The first section, therefore, becomes purely reactive and dissipates little or no acoustical energy. For example, with $kb = 6$, the first section accounts for a transmission loss of only 0.8 dB, whereas for the second section the loss is about 14.4 dB. Hence, the second section produces almost twice as much loss as does the corresponding optimal uniform liner, which is twice as long. At the present time, it is thought that the first section (closest to the source) causes a modal redistribution of sound and thereby increases the effectiveness of the second section with an attendant increase in the overall loss of acoustical energy. (See refs. 7 and 8.)

Also note that for $kb > 10$, the uniform and two-section configurations give essentially the same transmission loss. It would seem that at these frequencies, the two-section solutions, which were started at the optimal uniform solutions, would remain stationary. To the contrary, however, the DFP algorithm located an optimum with substantially different admittances. For example, with $kb = 20$, the optimal uniform liner has $\beta = 0.14 - 0.32i$. With two sections, an optimum is found with $\beta = 0.02 - 0.34i$ for the first section and $\beta = 0.29 - 0.48i$ for the second. Thus, it is clear that the transmission loss is close to its maximum value over a fairly large region in the four-dimensional admittance space.

Monopole source.- Results are presented in figure 10 and table VI for a monopole source located in a duct with an impedance discontinuity (two sections). In general, the DFP algorithm was initialized at the admittance values of the corresponding optimal uniform liner configuration. A number of the cases, however, were started differently because of the numerical problems associated with calculating the eigenvalues of the radial modes.

Transmission losses for comparable two-section and uniform configurations are presented in figure 10(a). The largest advantage of liner segmentation appears in the lower frequency range $kb \leqq 7$. It should be recalled that like

results were obtained for a plane-wave source. Also it is interesting to note that at these lower frequencies ($kb \leq 7$), where the two-section configuration is superior, only the lowest two radial modes are cut on. At the higher frequencies ($kb \geq 7$), the transmission losses for the uniform and segmented liner configurations converge to a constant loss of about 10 dB. However, although the uniform liner settles down to this constant value at about $kb = 7$, the segmented liner displays two intervals of significant additional loss, near $kb = 11$ and $kb = 13$. These bumps in the curve are probably associated with the cut on of higher order radial modes, which are strongly excited by the monopole source.

Optimal admittance values are presented in figures 10(b) and 10(c). The high-frequency values are in good agreement with the predictions of the single reflection criterion as discussed earlier. This geometric acoustics approximation gives optimal admittances of approximately $0.8 + \frac{0.6i}{kb}$ and $0.6 + \frac{0.4i}{kb}$ for the first and second sections, respectively. The second section admittance is very close to its high-frequency limit for $kb > 7$, but the first section does not settle down near its limit until $kb > 17$. In fact, the first section admittance curve has about the same shape as does the plot of the corresponding optimal uniform liner admittance (see fig. 6) for $kb > 7$, but is more exaggerated. Here, the average of the two-section admittances is approximately equal to the optimal uniform admittance, but this may be a result of taking the uniform optimum as the initial guess for the segmented liner optimization. Different curves resulted for different liner admittance starting values. In fact, the liner properties for this duct and source configuration were found to be very sensitive to the starting values used with the DFP algorithm. However, the maximum transmission loss for $kb > 7$ appeared to remain relatively stationary and varied only slightly from the values shown in figure 10(a). Nonetheless, figure 10 does suggest that when several propagating modes are excited by the noise source, a simplified ray approach may be adequate for selecting the admittances of sections not adjacent to the source. A full mode theory would still be required at lower frequencies and even at intermediate frequencies for the section closest to the source.

Turbomachinery Source

A 0.3048-m-diameter research compressor installed in an anechoic chamber at Langley Research Center was selected as the noise source to be modeled for the calculations presented in this section. The compressor was configured as a single stage with 19 rotor blades and 26 outlet guide vanes. The flow condition corresponding to a shaft speed of about 19 000 rpm was selected. For this situation the average axial flow Mach number in the inlet is approximately 0.4 and the normalized blade passage frequency is $kb = 16.53$, where b is the inlet radius. The various physical parameters for the compressor configuration were supplied to a computer program (ref. 15) which calculated the source mode amplitudes and phase angles for rotor/stator interaction noise. The source program employs the Kemp-Sears viscous-wake interaction model. According to the usual Tyler-Sofrin analysis, three $m = -7$ radial modes are excited, that is, $(-7,0)$, $(-7,1)$, and $(-7,2)$.

Results for the finite-length liner configurations shown in figure 11 are summarized in figure 12. The numerical optimization process was initialized at $\theta = 5.0$ and $kd = 1.57$ for all lined sections. The bar labeled "exact" in figure 12 shows the maximum transmission loss for the exact modal source structure. Although for the plane-wave and monopole sources very little was gained from liner segmentation at a kb as large as 16, for this particular turbomachinery source an additional 3 dB of attenuation can be realized with two liner segments and 5 dB with three segments.

The other bars in figure 12 correspond to variations from the exact source structure. Calculations were made for one-, two-, and three-segment liners for each of the following source variants: (1) assuming equal energy in each of the propagating $m = -7$ modes with the calculated relative phasing retained, (2) replacing the three complex modal coefficients with their absolute values (zero phase), and (3) setting the amplitude of all but the least attenuated mode to zero. It is clear from this example that although liner segmentation can result in a significant improvement regardless of the source type, the liner cannot be optimally designed unless both the modal distribution of source energy and the relative phasing among these modes are known.

CONCLUSIONS

This paper has presented an investigation of the influence of source characteristics on the optimal properties of uniform and two-section ducts. Two simplified sources were considered in some detail and over a frequency range greater than previously studied. The principal findings of this study are:

(1) Optimal liners based on modal theory approach Cremer's criterion at low normalized frequencies; that is, $kb < 1$.

(2) Optimal liners based on modal theory approach the geometric acoustics limit at high normalized frequencies; that is, $kb > 10$.

(3) Source distribution effects are important for optimal liner design.

(4) Two-section liners are significantly better than one-section liners in the frequency range $3 \leq kb \leq 7$ for plane-wave and monopole sources.

(5) Source and termination impedance effects, although given only a limited examination in this paper, appear to be unimportant for optimal liner design.

Langley Research Center
National Aeronautics and Space Administration
Hampton, VA 23665
October 27, 1976

APPENDIX

OPTIMAL LINER DESIGN BY ASCENT ALGORITHMS

The purpose of this appendix is to summarize the general characteristics of the Davidon-Fletcher-Powell (DFP) optimization algorithm. The DFP algorithm is discussed extensively by Luenberger (ref. 10) and interested readers are encouraged to consult this reference for additional information. Some material, however, is provided in this appendix for the sake of completeness beginning with the method of constant transmission loss contours.

Method of Transmission Loss Contours

When the admittance space is two-dimensional, as is the case for a uniform or one-section liner (fig. 3, for example), optimal liner admittance values can be determined by plotting constant transmission loss contours. Typical results are shown in figure 5 for a plane-wave source with $L = 2b$. Shown in figures 5(a) and 5(b) are the contours for a uniform liner (fig. 3) with $kb = 2$ and $kb = 3$, respectively. The real part of the admittance ζ (the conductance) is plotted along the abscissa whereas the imaginary part of the admittance σ (the susceptance) is plotted along the ordinate. The transmission loss contours of $TL = 10, 15, 20, \ldots$ represent the locus of points in the admittance plane yielding 10, 15, 20, . . . dB, respectively, of noise attenuation. The contours shown here were constructed by computing the losses at 100 grid points and using a computer-graphics program to map the contours. An alternative numerical approach, which is applicable with the higher dimensional admittance spaces of multisectioned liners, is discussed in the next section.

The DFP Method

Refer to figure 13 and let an arbitrary point in the admittance plane be determined by the admittance vector $\bar{B}$ with components (ζ,σ). (See eq. (6).) The basic strategy of the DFP method is intimately associated with the definition of an ascent vector $\bar{D}$. Thus, in figure 13 by starting at an arbitrary initial point (initial feasible solution) $\bar{B}_0$ in the admittance plane, it is desired to move in a direction specified by the ascent vector $\bar{D}_0$ so that a greater value of transmission loss TL is obtained at $\bar{B}_1$. This approach suggests the following iterative algorithm:

$$\bar{B}_{k+1} = \bar{B}_k + \alpha_k \bar{D}_k \qquad (k = 0, 1, 2, \ldots) \qquad (A1)$$

determined by a sequence of ascent vectors $\bar{D}_0, \bar{D}_1, \ldots, \bar{D}_k$, each leading to a greater value of TL. The sequences of α_k parameters appearing in equations (A1) are scalars which maximize TL_{k+1}. Here the subscript k indicates the kth iteration.

APPENDIX

To be more specific, in the DFP method the ascent vectors D_k are chosen to be

$$\bar{D}_k = [S_k]\,\overline{\nabla\{TL\}}_k \tag{A2}$$

where $[S_k]$ is a square matrix and $\overline{\nabla\{TL\}}_k$ is the gradient of TL evaluated at $\bar{B}_k$. The square matrix $[S_k]$ is updated at each iteration in an attempt to have the algorithm converge more rapidly than the method of steepest ascent - in which case $[S_k]$ is always the identity matrix - and in an attempt to be computationally more efficient than Newton's method - in which case $[S_k]$ is always the inverse of the matrix of second partials of TL.

The DFP algorithm, as given by Luenberger (ref. 10), is as follows:

(1) Start with any symmetric positive-definite matrix $[S_0]$ (usually $[S_0] = [I]$) and any initial point $\bar{B}_0$.

(2) Beginning with $k = 0$, set

$$\bar{D}_k = [S_k]\,\overline{\nabla\{TL\}} \tag{A3a}$$

(3) Maximize $TL\left(\bar{B}_k + \alpha_k \bar{D}_k\right)$ with respect to α_k to obtain

$$\bar{B}_{k+1} = \bar{B}_k + \alpha_k \bar{D}_k \tag{A3b}$$

(4) With $\bar{P}_k = \alpha_k \bar{D}_k$, set $\bar{R}_k = \overline{\nabla\{TL\}}_{k+1} - \overline{\nabla\{TL\}}_k$ and determine the updated $[S_{k+1}]$ matrix as follows:

$$[S_{k+1}] = [S_k] + \frac{\bar{P}_k \bar{P}_k^T}{\bar{P}_k^T \bar{R}_k} - \frac{[S_k]\bar{R}_k \bar{R}_k^T [S_k]}{\bar{R}_k^T [S_k] \bar{R}_k} \tag{A3c}$$

and repeat the procedure by going to step (2). The procedure is terminated when $\bar{D}_k^T \bar{D}_k$ is sufficiently small.

The DFP method combines the best features of steepest ascent (good performance if the initial value of $\bar{B}_0$ is not close to the solution) and Newton's method (rapid convergence close to the solution). It is generally conceded to be a fast, reliable optimization method and it works very well on problems of the type considered in this report.

REFERENCES

1. Cremer, Lothar: Theorie der Luftschall-Dämpfung im Rechteckkanal mit schluckender Wand und das sich dabei ergebende höchste Dämpfungsmass. Acoustica, vol. 3, no. 2, 1953, pp. 249-263.

2. Rice, Edward J.: Attenuation of Sound in Soft-Walled Circular Ducts. Aerodynamic Noise, Univ. of Toronto Press, c.1969, pp. 229-249.

3. Tester, B. J.: The Optimization of Modal Sound Attenuation in Ducts, in the Absence of Mean Flow. J. Sound & Vib., vol. 27, no. 4, Apr. 22, 1973, pp. 477-513.

4. Wilkinson, J. P. D.: The Calculation of Optimal Linings for Jet Engine Inlet Ducts - Part II. NASA CR-1832, 1971.

5. Lansing, D. L.; and Zorumski, W. E.: Effects of Wall Admittance Changes on Duct Transmission and Radiation of Sound. J. Sound & Vib., vol. 27, nc. 1, Mar. 8, 1973, pp. 85-100.

6. Quinn, Dennis W.: Attenuation of the Sound Associated With a Plane Wave in a Multisectional Duct. AIAA Paper No. 75-496, Mar. 1975.

7. Beckemeyer, Roy J.; and Sawdy, David T.: Optimization of Duct Acoustic Liners of Finite Length. Paper H1, 89th Meeting Acoust. Soc. America (Austin, Texas), Apr. 1975.

8. Sawdy, David T.; Beckemeyer, Roy J.; and Patterson, John D.: Optimum Segmented Acoustic Liners for Flow Ducts. Paper D6, 90th Meeting Acoust. Soc. America (San Francisco, Calif.), Nov. 1975.

9. Zorumski, William E.: Acoustic Theory of Axisymmetric Multisectioned Ducts. NASA TR R-419, 1974.

10. Luenberger, David G.: Introduction to Linear and Nonlinear Programming. Addison-Wesley Pub. Co., Inc., c.1973.

11. Cantrell, R. H.; and Hart, R. W.: Interaction Between Sound and Flow in Acoustic Cavities: Mass, Momentum, and Energy Considerations. J. Acoust. Soc. America, vol. 36, no. 4, Apr. 1964, pp. 697-706.

12. Zorumski, William E.; and Mason, Jean P.: Multiple Eigenvalues of Sound-Absorbing Circular and Annular Ducts. J. Acoust. Soc. America, vol. 55, no. 6, June 1974, pp. 1158-1165.

13. Cremer, L.: The Second Annual Fairey Lecture: The Treatment of Fans as Black Boxes. J. Sound & Vib., vol. 16, no. 1, May 8, 1971, pp. 1-15.

14. Morse, Philip M.; and Ingard, K. Uno: Theoretical Acoustics. McGraw-Hill Book Co., Inc., c.1968.

15. Clark, T. L.; Ganz, U. W.; Graf, G. A.; and Westall, J. S.: Analytic Models of Ducted Turbomachinery Tone Noise Sources. NASA CR-132443, 1974.

TABLE I.- OPTIMAL PROPERTIES OF A UNIFORM CIRCULAR LINER (FIG. 3)

FOR A PLANE-WAVE SOURCE AND L = 2b

kb	Conductance, ξ	Susceptance, σ	TL, dB
2	1.54	1.29	49.8
3	.81	.78	31.5
4	.46	.61	15.1
5	.34	.59	9.8
6	.28	.57	7.6
8	.22	.53	5.4
10	.21	.45	4.5
12	.19	.40	4.1
14	.17	.38	3.7
16	.15	.36	3.3
18	.15	.33	3.0
20	.14	.32	2.9

TABLE II.- OPTIMAL PROPERTIES OF A UNIFORM CIRCULAR LINER (FIG. 3)

FOR A MONOPOLE SOURCE AND L = 2b

kb	Conductance, ξ	Susceptance, σ	TL, dB
2	1.11	1.16	43.5
2.5	.82	.80	37.7
3	.62	.53	30.5
3.5	.49	.29	23.0
4	.45	.07	16.9
4.5	.48	-.12	12.9
5	.58	-.26	10.8
5.5	.79	-.34	9.7
6	1.08	-.18	9.7
6.5	.98	.14	9.8
7	.76	.17	10.3
7.5	.68	.13	10.5
8	.62	.07	10.3
8.5	.60	.01	10.1
9	.63	-.03	9.8
9.5	.65	.01	9.7
10	.51	.11	10.3
10.5	.45	-.10	10.5
11	.68	-.22	9.9
11.5	.85	-.09	9.5
12	.84	.05	9.4
12.5	.71	.20	9.6
13	.59	.18	10.3
13.5	.50	.05	10.7
14	.51	-.05	10.5
14.5	.60	-.15	10.0
15	.76	-.16	9.5
15.5	.88	-.03	9.5
16	.78	.17	9.7
16.5	.62	.10	10.1
17	.61	.01	10.1
17.5	.63	.01	9.9
18	.62	-.01	9.7
18.5	.65	-.04	9.5
19	.69	0	9.5
19.5	.64	.03	9.8
20	.63	-.04	9.9

TABLE III.- EFFECT OF SOURCE IMPEDANCE ON OPTIMAL PROPERTIES OF A UNIFORM CIRCULAR LINER (FIG. 11(a)) FOR L = 2b

(a) Plane-wave source

kb	Conductance, ξ	Susceptance, σ	TL, dB	Insertion loss, dB
2	1.47	1.13	66.6	67.1
3	.84	.69	49.7	49.8
4	.42	.55	13.1	13.2
6	.27	.54	7.0	7.0
8	.22	.50	4.7	4.7
10	.20	.42	4.1	4.1
14	.17	.37	3.4	3.4
18	.14	.33	2.9	2.9

(b) Uniform pressure source

kb	Conductance, ξ	Susceptance, σ	TL, dB	Insertion loss, dB
2	1.48	1.20	60.7	59.7
3	.86	.74	55.9	55.3
4	.45	.61	15.0	14.6
6	.29	.54	7.9	7.5
8	.21	.53	5.3	5.2
10	.20	.44	4.5	4.4
14	.17	.38	3.7	3.5
18	.15	.33	3.0	3.0

(c) Uniform velocity source

kb	Conductance, ξ	Susceptance, σ	TL, dB	Insertion loss, dB
2	1.43	1.08	73.9	76.0
3	.82	.68	51.9	51.5
4	.41	.53	12.5	12.8
6	.28	.54	6.0	6.4
8	.22	.45	4.3	4.4
10	.21	.41	3.8	3.9
14	.16	.36	3.2	3.4
18	.14	.32	2.7	2.8

TABLE IV.- EFFECT OF TERMINATION IMPEDANCE ON OPTIMAL PROPERTIES OF A UNIFORM CIRCULAR LINER (FIG. 11(a)) FOR L = 2b

[Uniform pressure source]

kb	Radiation termination			$Z_{m\mu}$ = 1.0 (eq. (20))			Z_t = 1.0 (ref. 6)		
	Conductance, ξ	Susceptance, σ	IL, dB	Conductance, ξ	Susceptance, σ	IL, dB	Conductance, ξ	Susceptance, σ	IL, dB
1.57	2.40	3.20	53.1	1.86	3.30	41.6	2.40	3.20	43.0
4.72	.39	.61	10.8	.39	.61	10.6	.38	.58	11.7
7.85	.25	.51	5.4	.25	.50	5.6	.23	.57	6.2
12.57	.22	.36	3.9	.22	.35	3.9	.24	.30	4.1

TABLE V.- OPTIMAL PROPERTIES OF A TWO-SECTION CIRCULAR LINER (FIG. 8)

FOR A PLANE-WAVE SOURCE AND L = 2b

kb	First section		Second section		TL, dB
	Conductance, ξ	Susceptance, σ	Conductance, ξ	Susceptance, σ	
2	1.48	1.44	1.54	1.01	53.2
2.5	1.09	1.06	1.12	.88	43.5
3	.75	.95	.97	.53	38.1
3.5	.42	.85	1.26	.25	38.4
4	.20	.78	1.40	.40	37.2
4.5	.07	.74	1.37	.60	36.2
5	.05	.70	1.02	.44	24.6
5.5	.04	.66	.92	.39	18.5
6	.04	.62	.82	.45	15.2
7	.03	.53	.53	.57	10.3
8	.02	.47	.48	.54	7.0
9	.02	.45	.40	.69	6.2
10	.02	.45	.59	.54	5.1
11	.02	.44	.60	.40	4.9
12	.01	.35	.54	.42	4.7
13	.01	.30	.48	.43	4.3
14	.02	.35	.29	.50	4.5
15	.02	.34	.29	.48	4.3
16	.02	.38	.40	.45	3.9
17	.01	.25	.38	.41	3.5
18	.01	.24	.36	.38	3.4
19	.12	.39	.16	.05	2.7
20	.16	.23	.23	.13	2.7

TABLE VI.- OPTIMAL PROPERTIES OF A TWO-SECTION CIRCULAR LINER (FIG. 8)

FOR A MONOPOLE SOURCE AND L = 2b

kb	First section		Second section		TL, dB
	Conductance, ξ	Susceptance, σ	Conductance, ξ	Susceptance, σ	
2	1.10	1.20	1.10	1.14	43.6
2.5	.60	.85	.81	.35	42.2
3	.32	.65	.01	-.05	47.4
3.5	.27	.28	.70	-.47	36.0
4	.17	-.02	1.39	-.97	35.9
4.5	.06	-.38	3.19	.46	37.1
5	.08	-.71	1.12	.87	44.9
5.5	0	-1.09	.85	.70	28.7
6	.13	-1.62	.70	.57	18.8
6.5	.63	-2.42	.60	.45	14.7
7	1.07	-.21	.48	.28	10.8
7.5	.76	-.12	.50	.29	11.0
8	.72	-.13	.51	.22	10.9
8.5	.65	-.19	.51	.13	10.5
9	.65	-.50	.55	.24	10.4
9.5	.65	-.11	.58	-.03	9.8
10	.33	.06	.64	.14	10.5
10.5	.11	-.25	.66	.08	13.9
11	.14	-.95	.60	.03	13.4
11.5	.96	-1.11	.64	.15	11.2
12	2.06	.20	.53	.06	10.7
12.5	1.14	.42	.47	.04	10.5
13	.29	.44	.70	-.05	11.5
13.5	.14	.01	.72	.04	12.0
14	.39	-.17	.61	.07	11.0
14.5	.72	-.45	.55	0	10.6
15	1.04	-.68	.51	-.01	10.4
15.5	1.17	-.41	.44	.06	10.3
16	1.28	.15	.50	0	10.3
16.5	.88	.18	.59	.04	10.2
17	.81	-.05	.50	.02	10.2
17.5	.76	.01	.50	.02	10.0
18	.73	-.02	.50	0	9.8
18.5	.74	-.10	.54	0	9.6
19	.84	-.05	.50	.06	9.6
19.5	.74	.01	.56	.01	9.8
20	.61	-.16	.66	.09	10.0

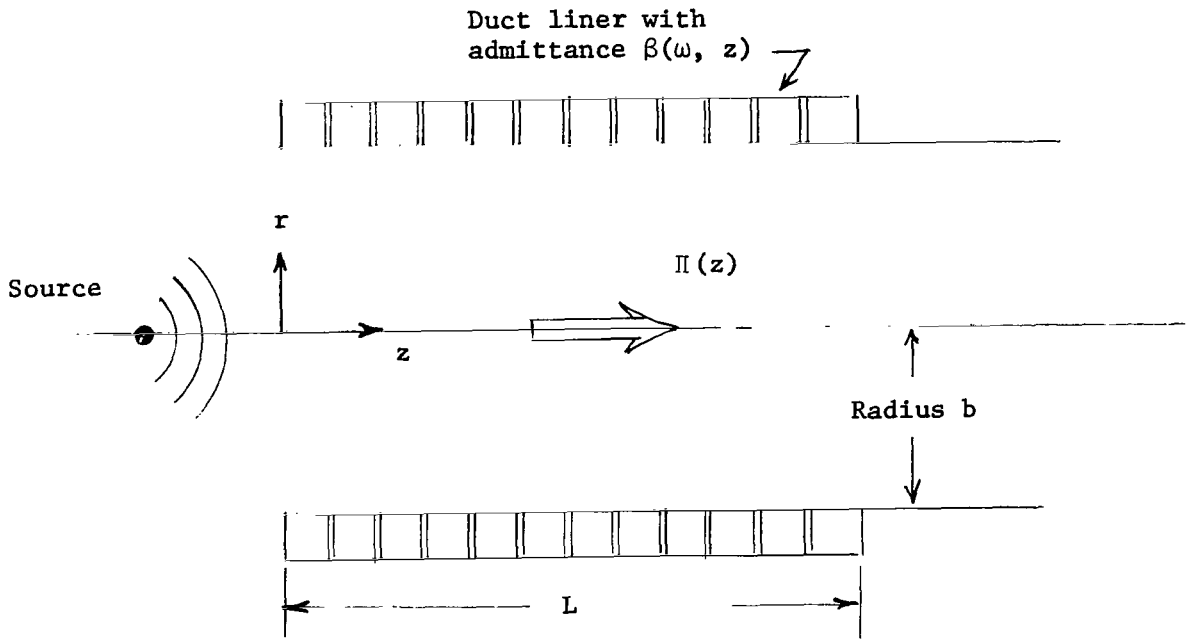

Figure 1.- Circular duct.

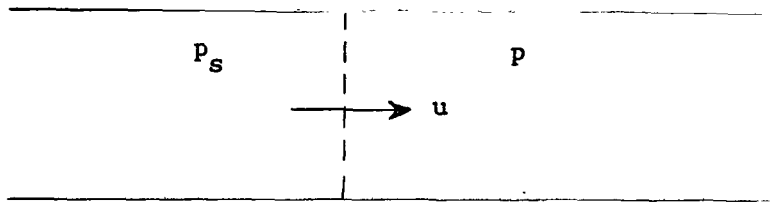

$$Z_s = \frac{p_s - p}{u}$$

(a) Pressure source.

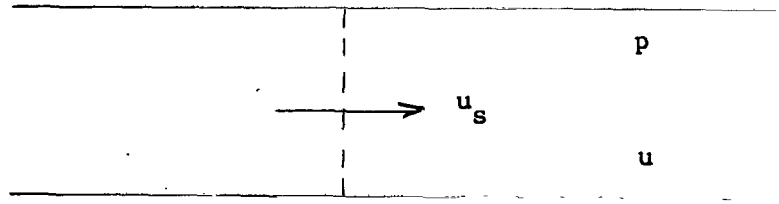

$$\beta_s = \frac{u_s - u}{p}$$

(b) Velocity source.

Figure 2.- Simplified source models.

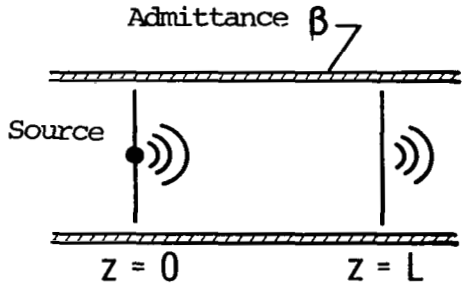

Figure 3.- Infinite duct with a uniform liner.

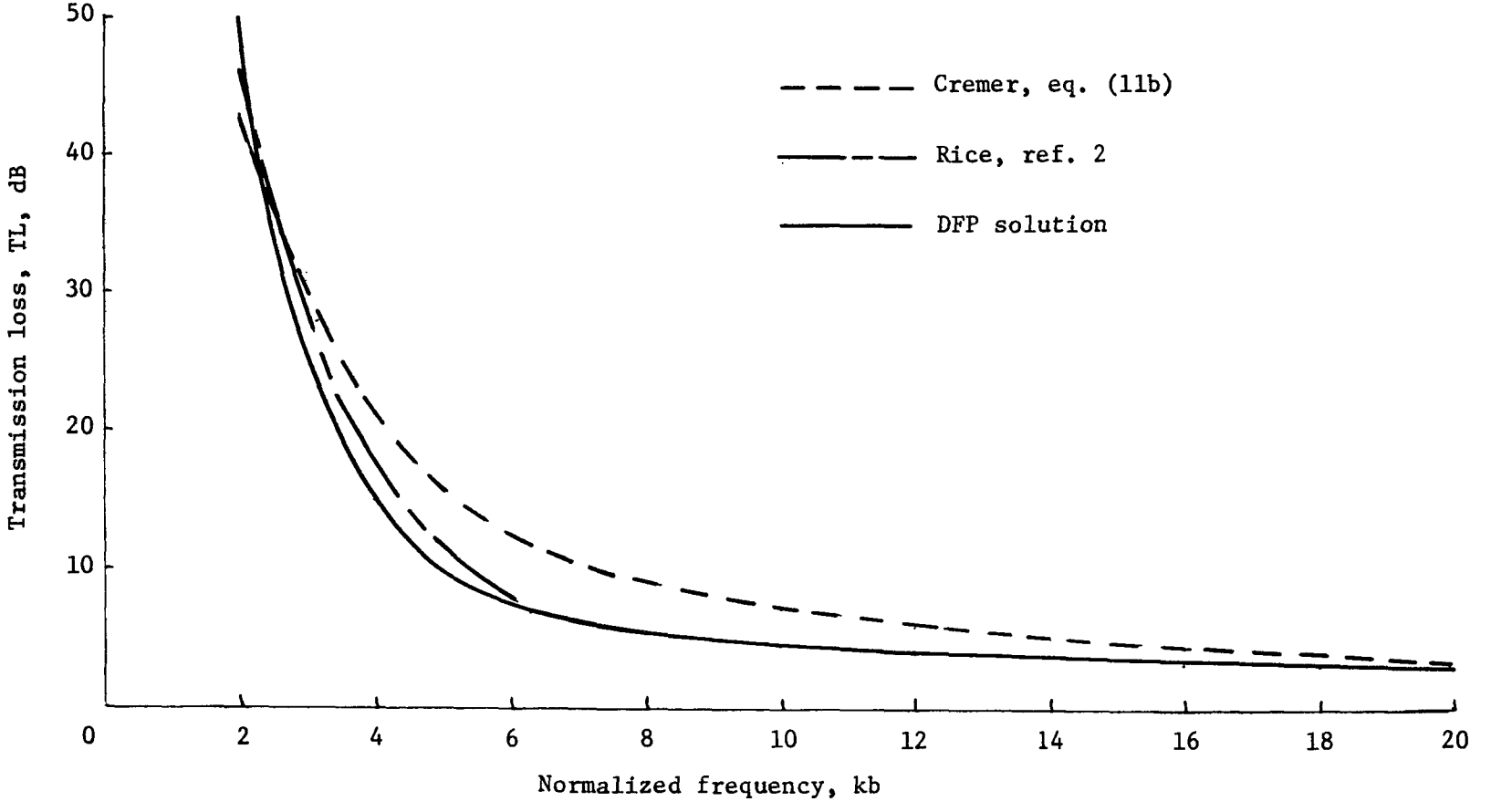

(a) Transmission loss.

Figure 4.- Optimal properties of a uniform circular liner (fig. 3) for a plane-wave source and L = 2b.

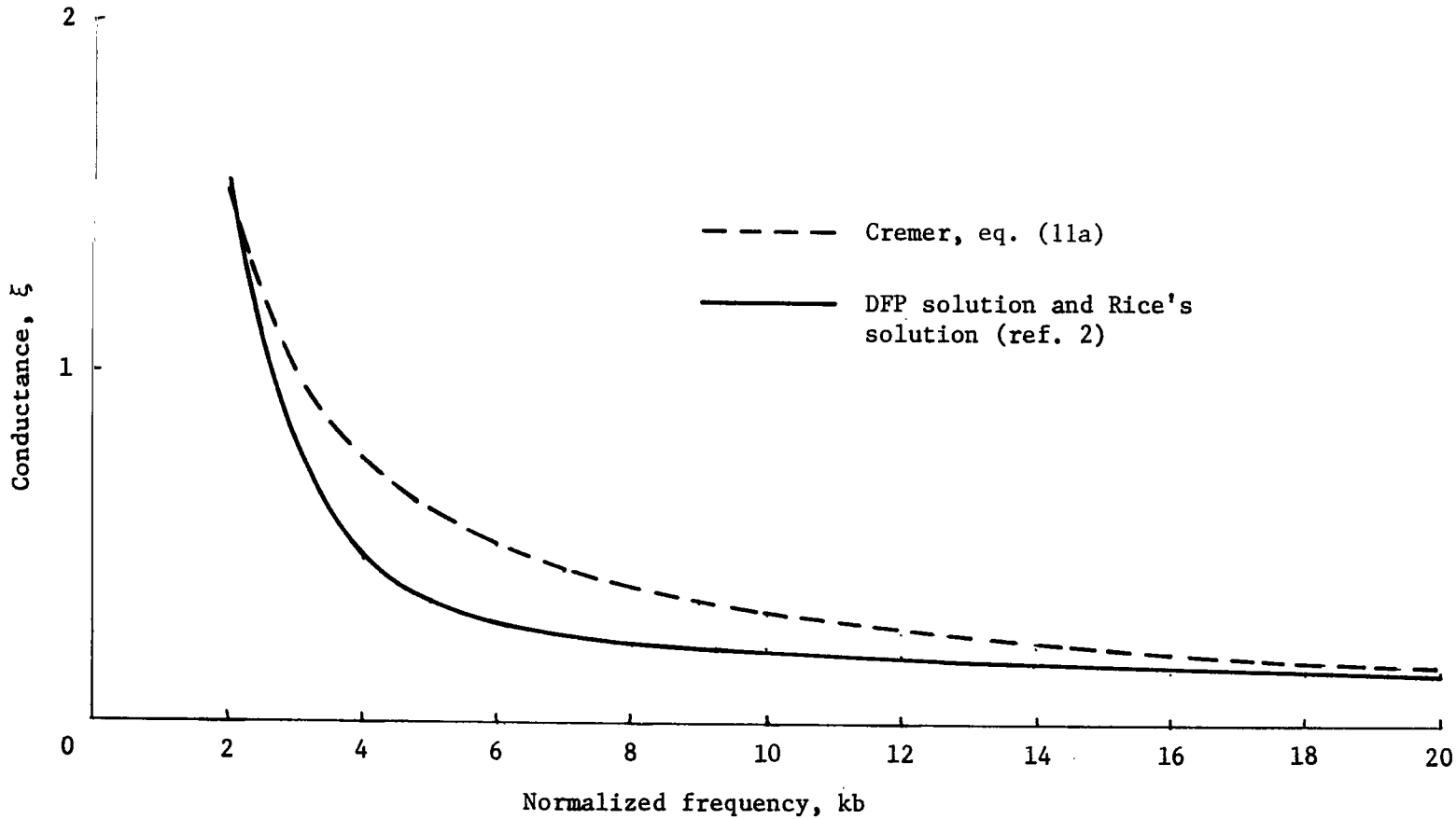

(b) Conductance.

Figure 4.- Continued.

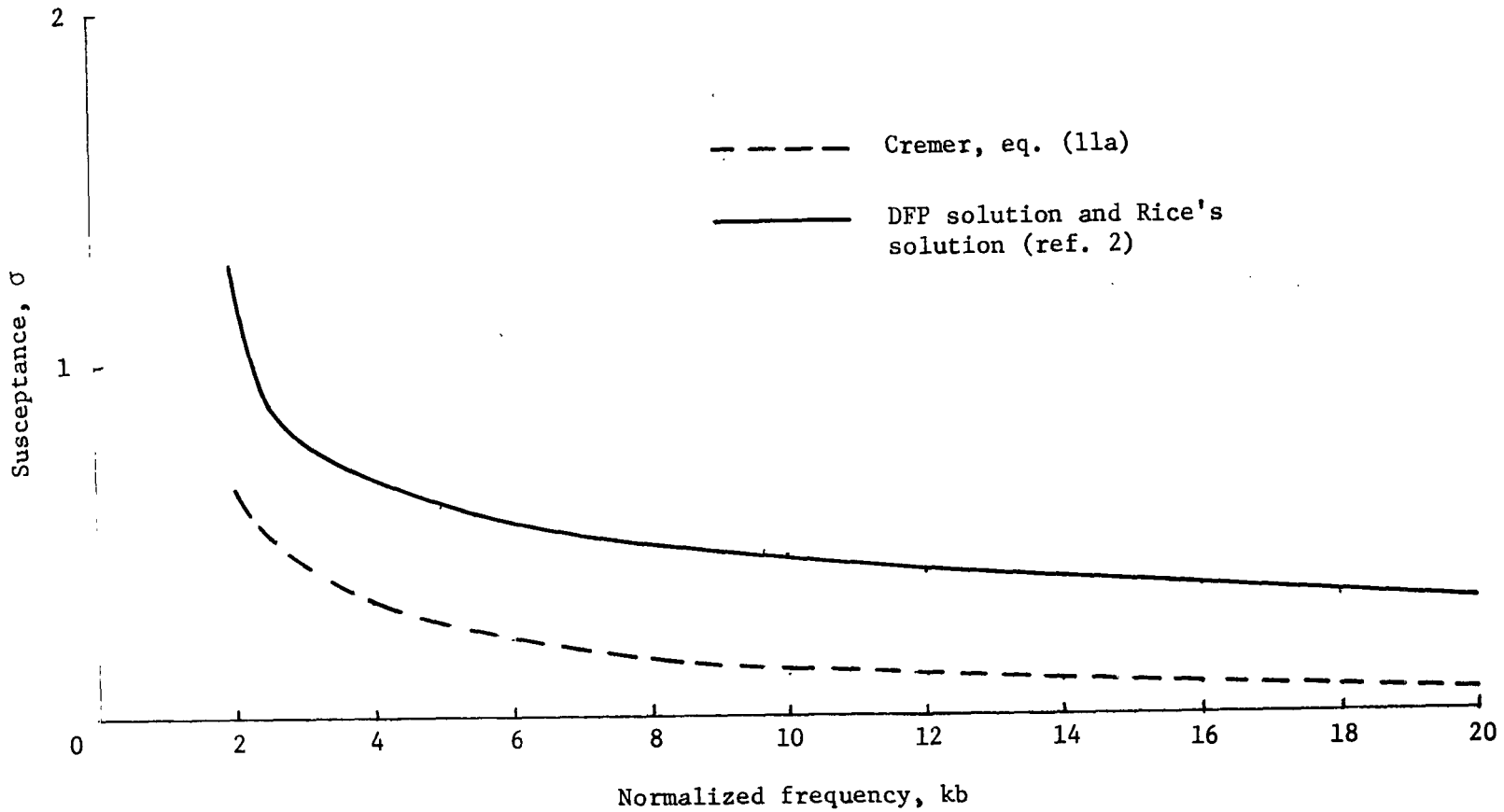

(c) Susceptance.

Figure 4.- Concluded.

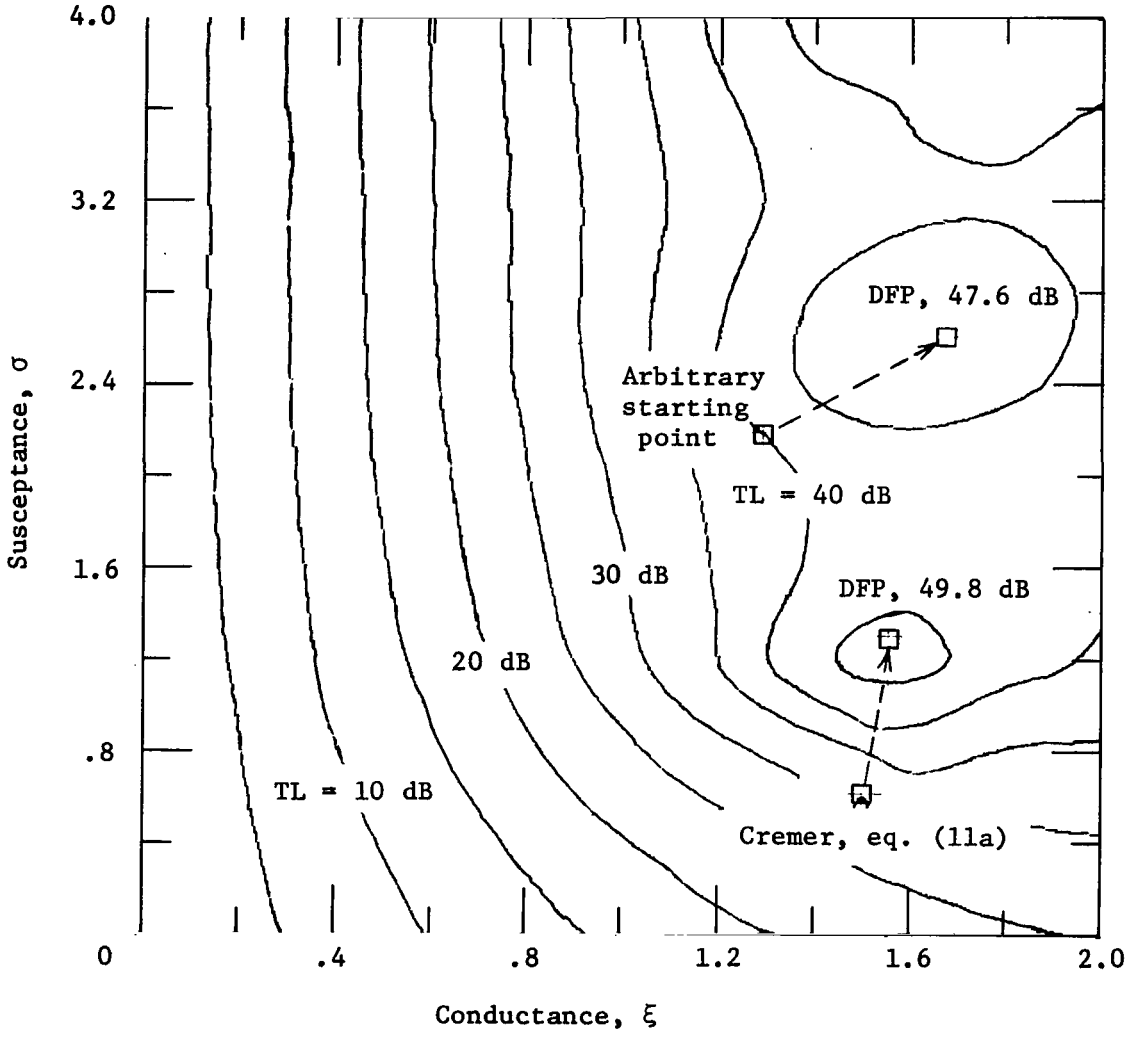

(a) kb = 2.0.

Figure 5.- Optimization by constant transmission loss contours for a uniform circular liner (fig. 3) with a plane-wave source and L = 2b.

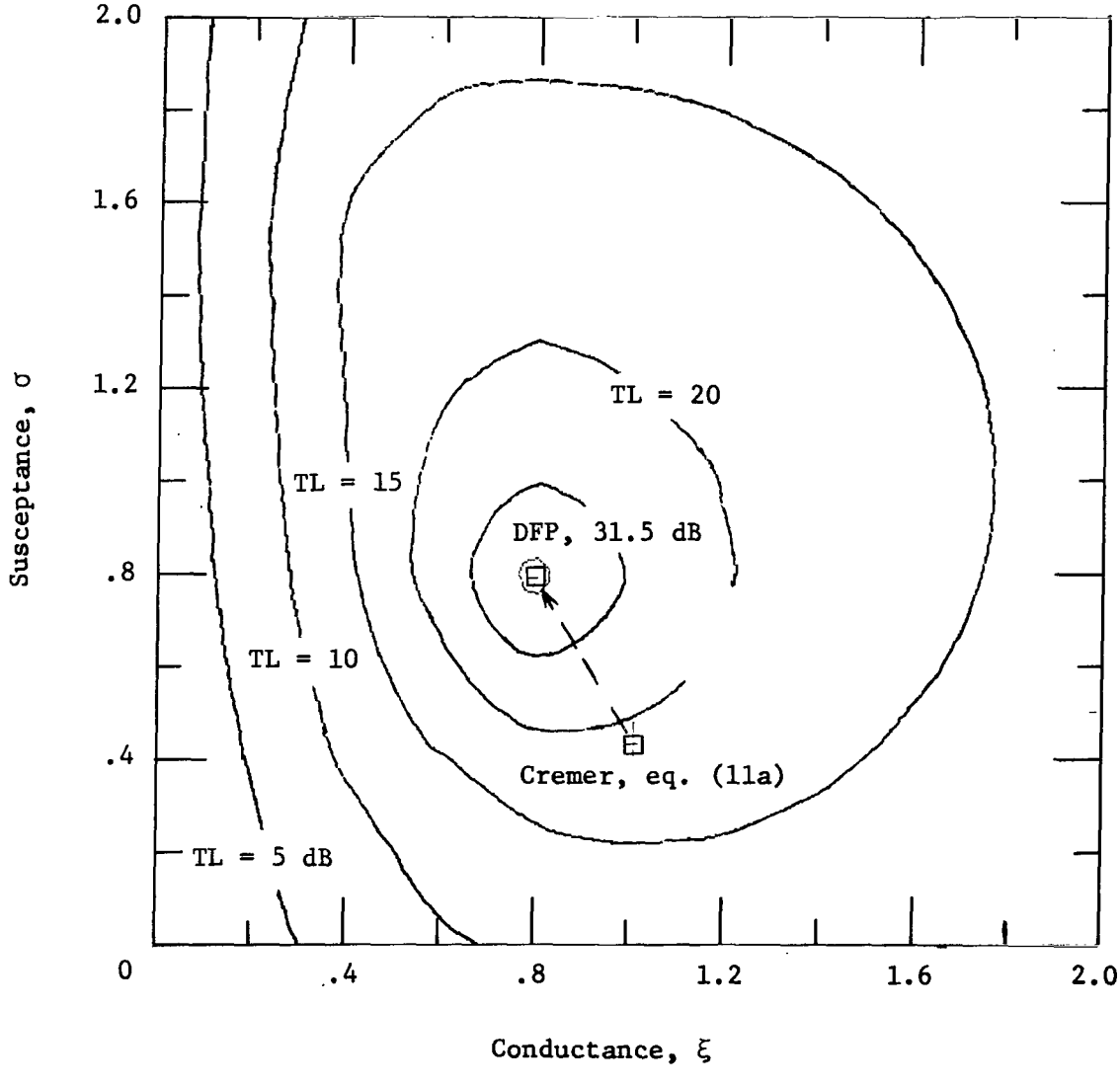

(b) kb = 3.0.

Figure 5.- Concluded.

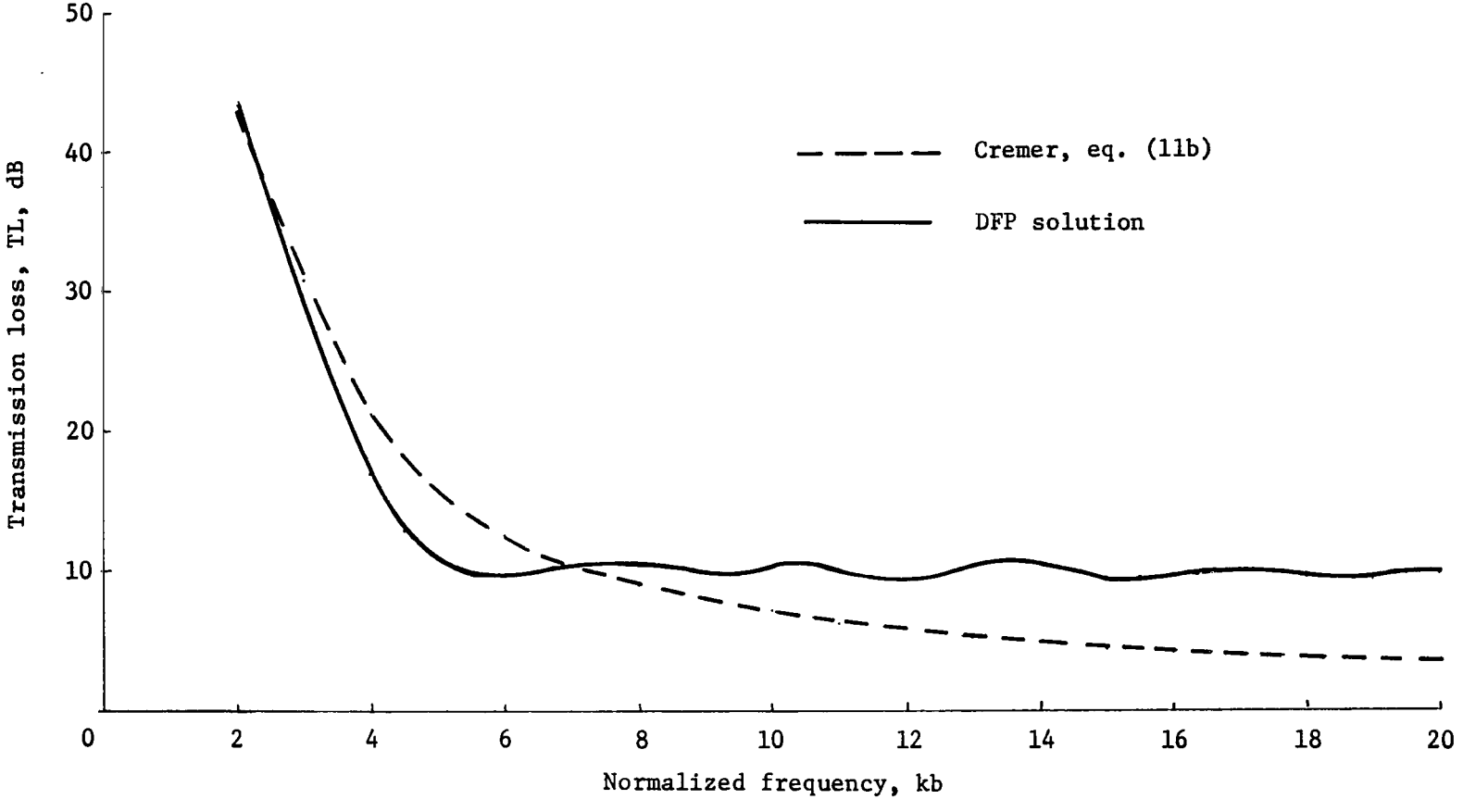

(a) Transmission loss.

Figure 6.- Optimal properties of a uniform circular liner (fig. 3) for a monopole source and $L = 2b$.

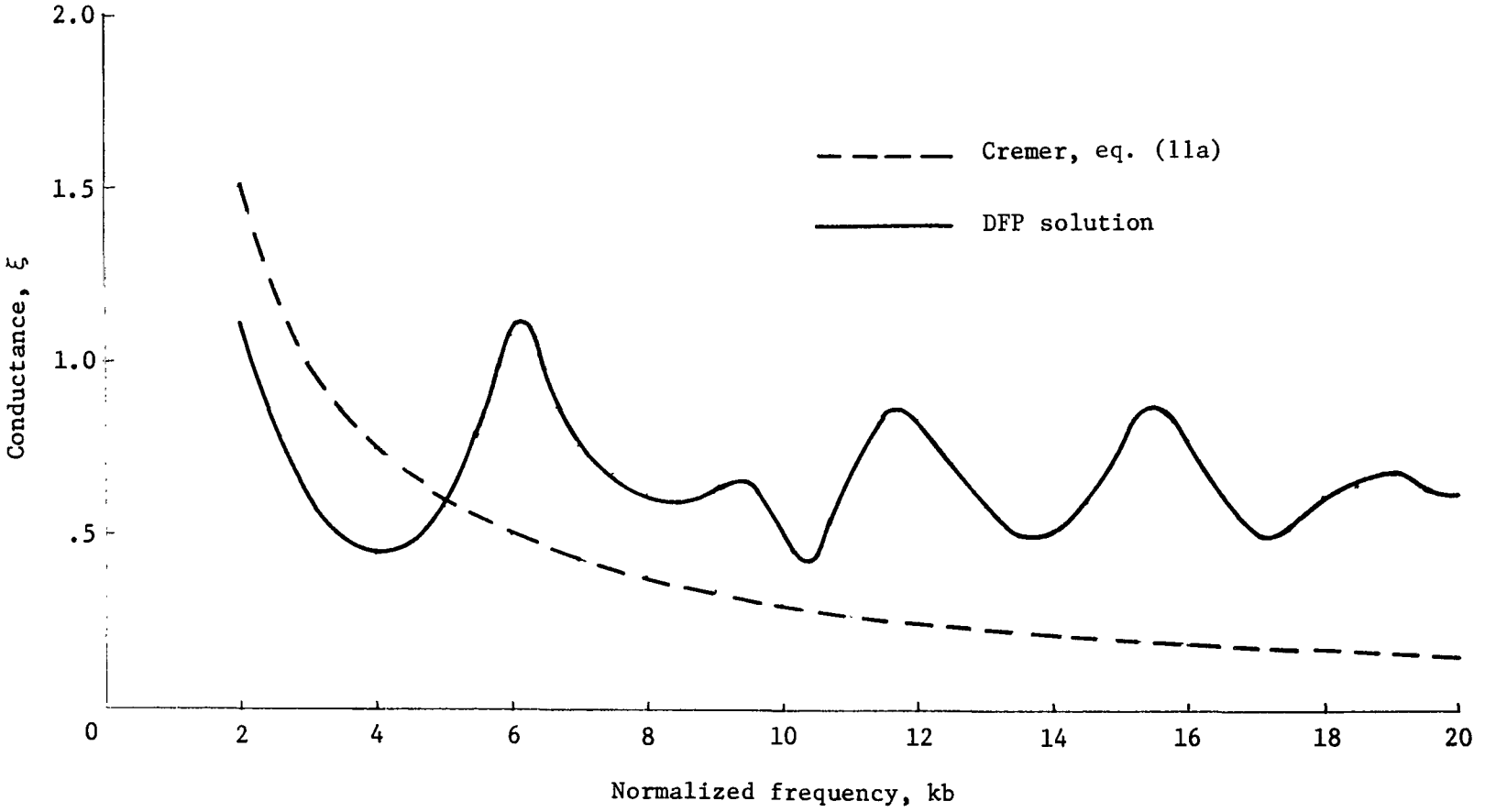

(b) Conductance.

Figure 6.- Continued.

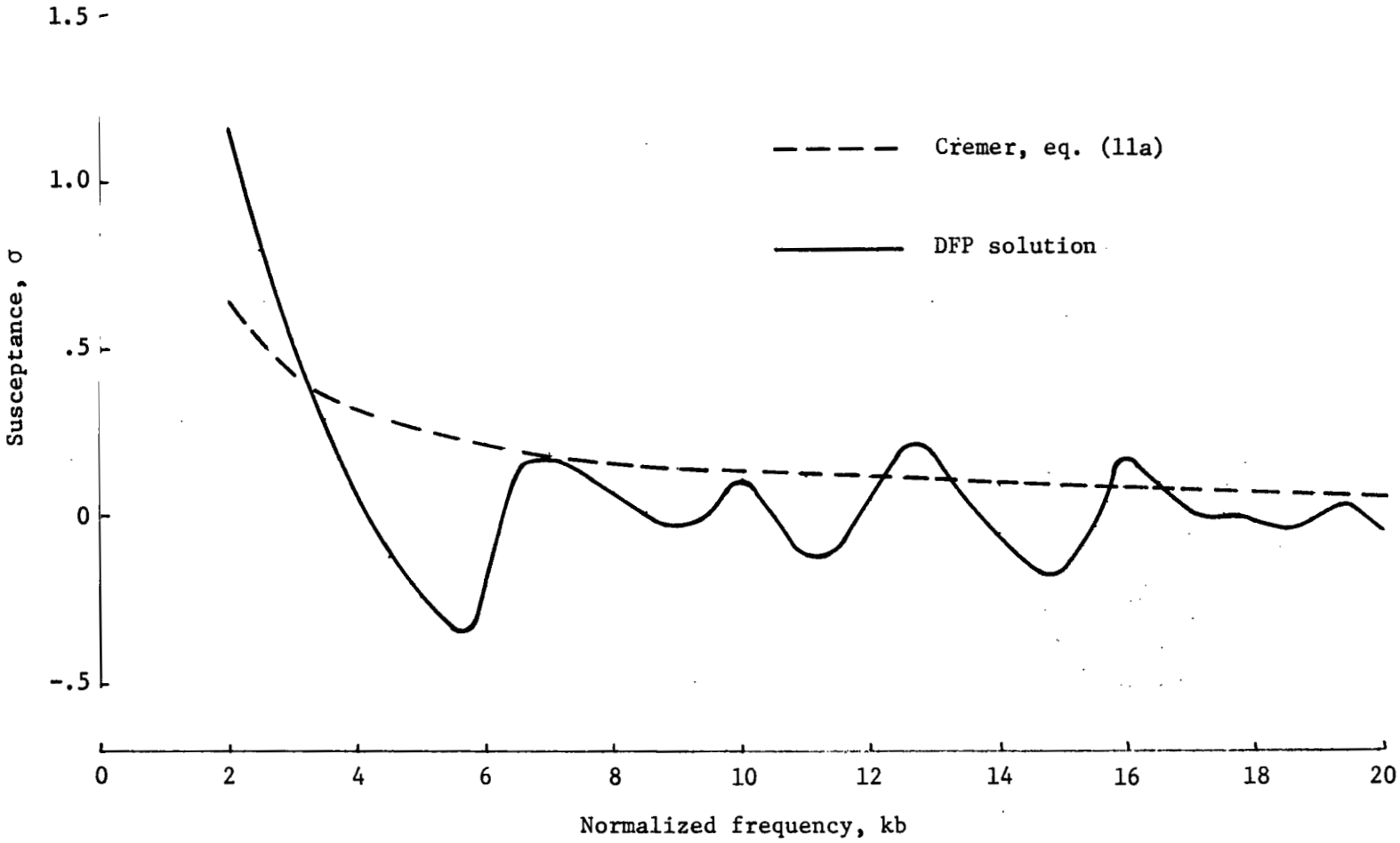

(c) Susceptance.

Figure 6.- Concluded.

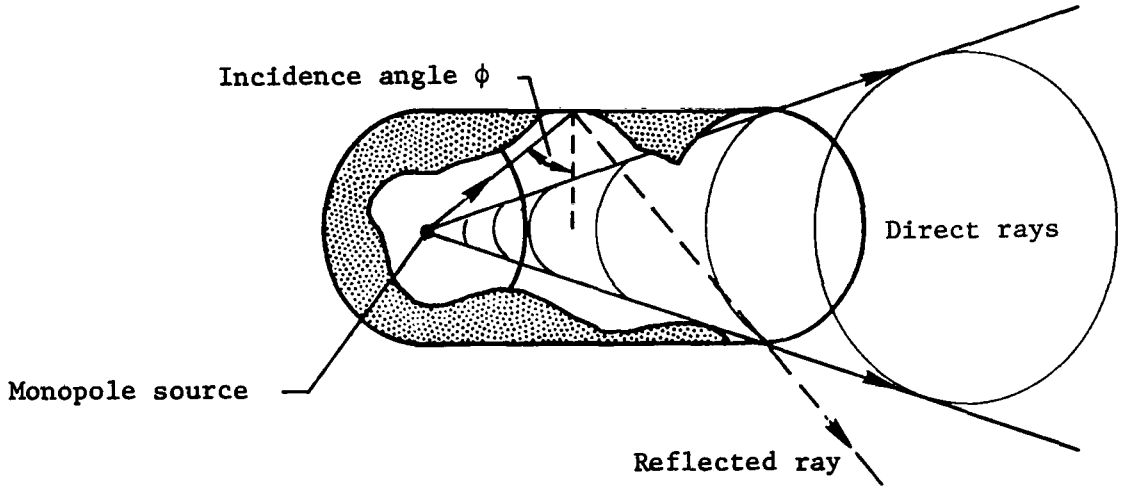

$$\text{Optimal normal admittance} = \left(1.0 + i\,\frac{\cos\phi}{kb}\right)\cos\phi$$

Figure 7.- Geometrical duct acoustics.

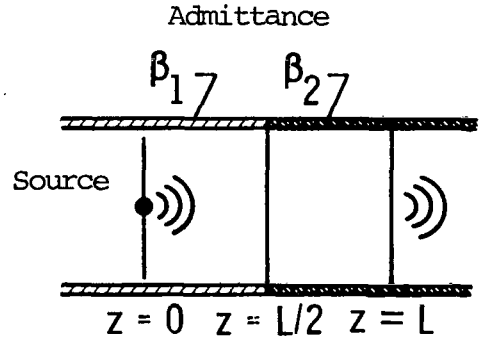

Figure 8.- Infinite duct with an admittance discontinuity.

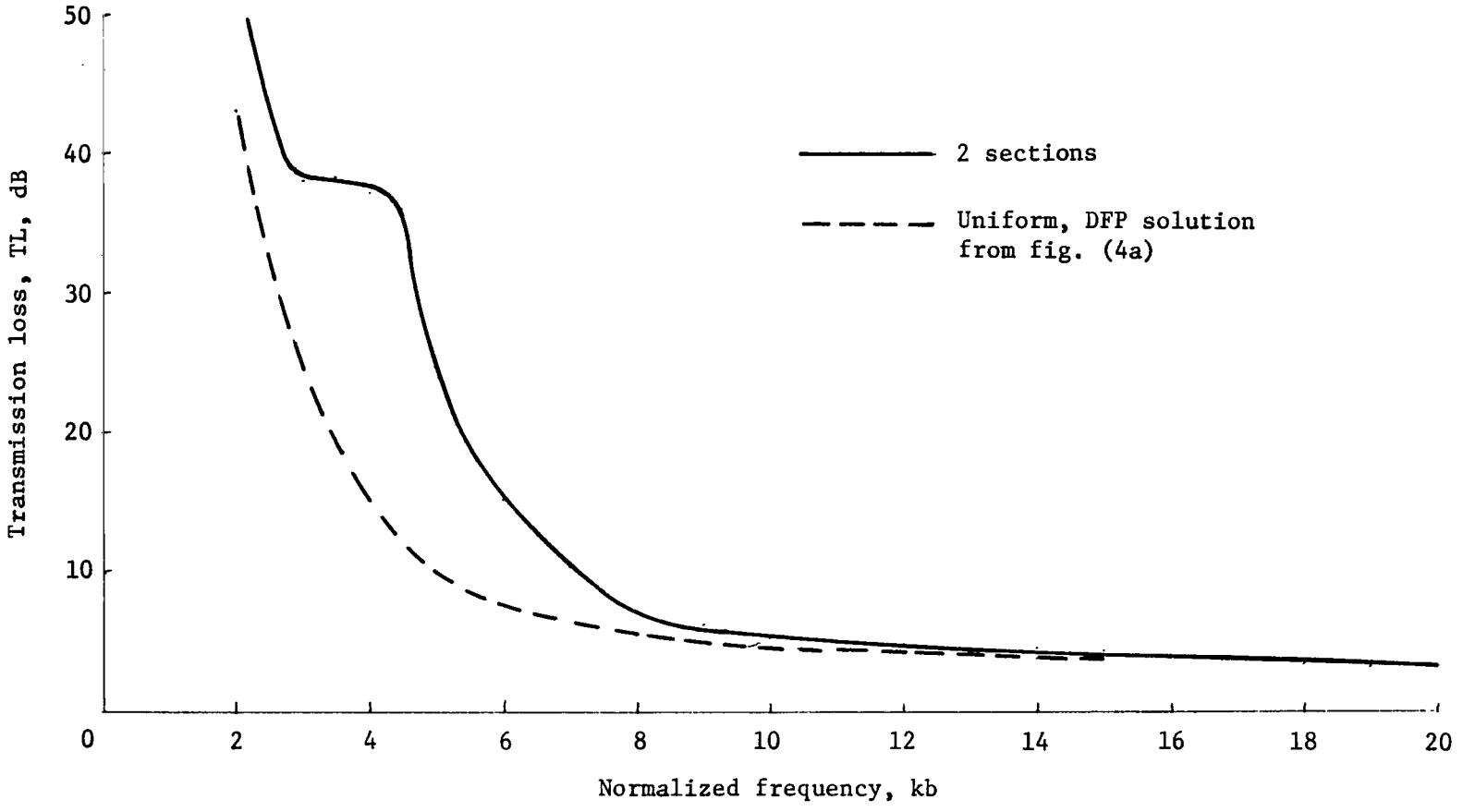

(a) Transmission loss.

Figure 9.- Optimal properties of a two-section circular liner (fig. 8) for a plane-wave source and L = 2b.

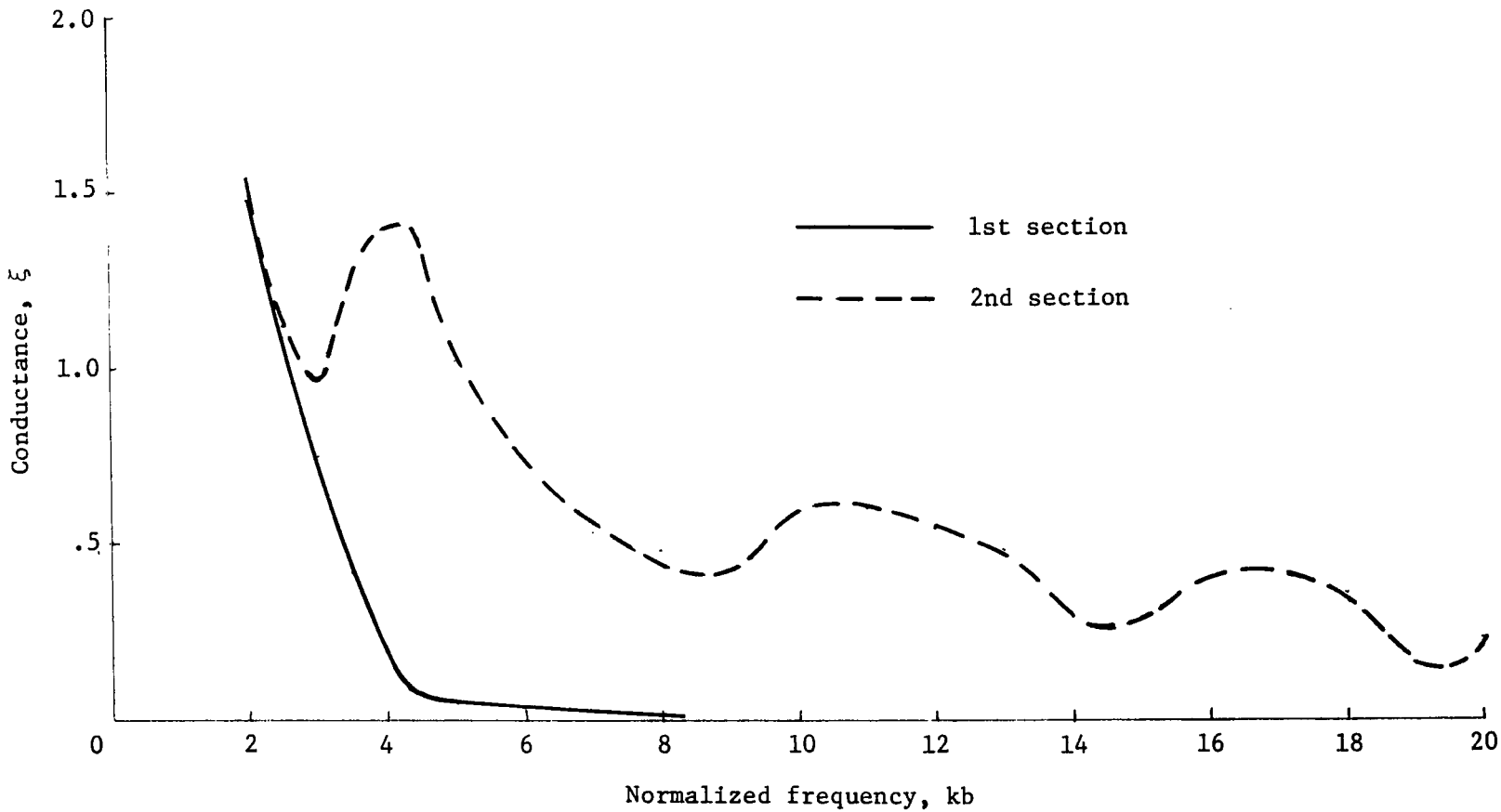

(b) Conductance.

Figure 9.- Continued.

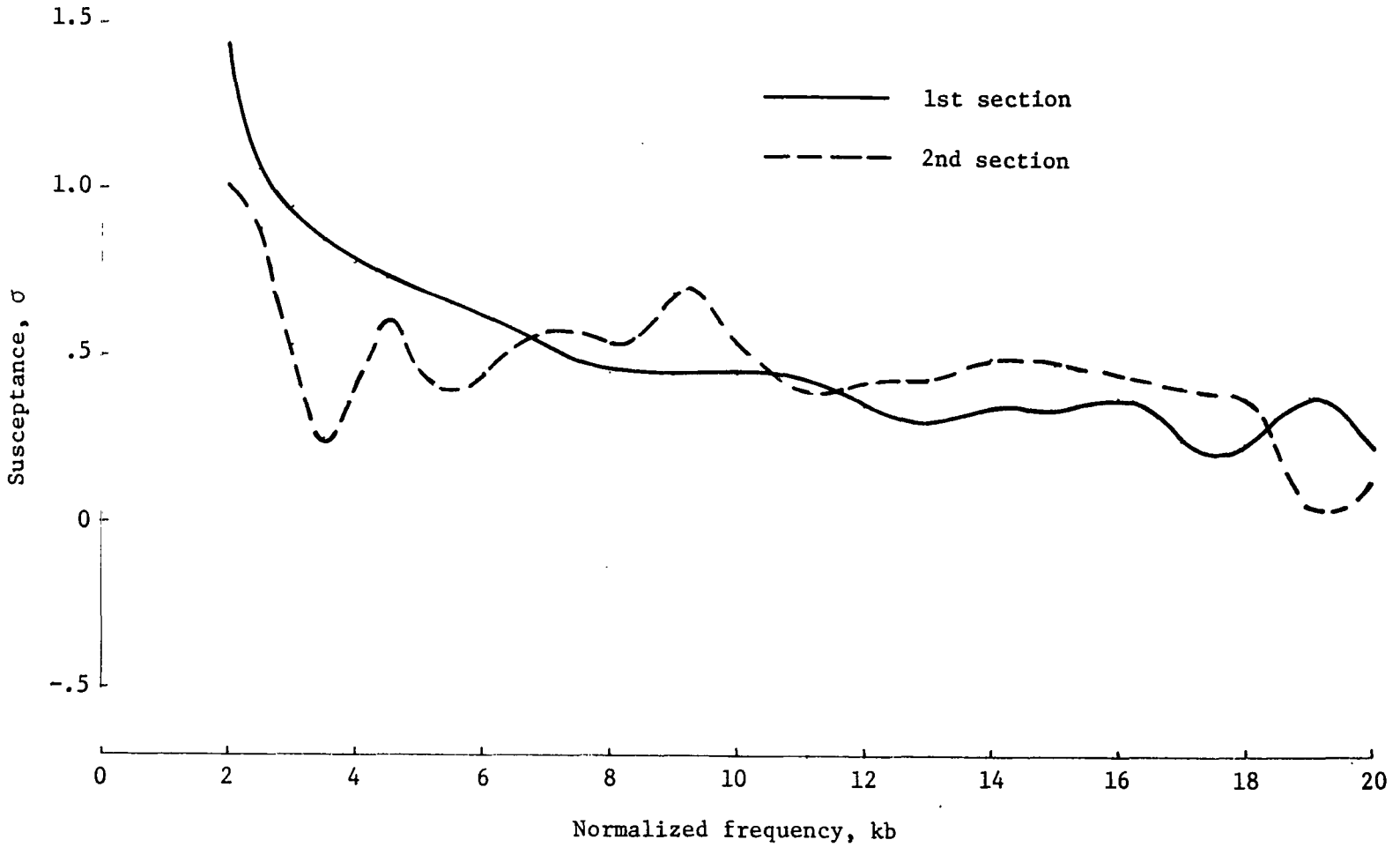

(c) Susceptance.

Figure 9.- Concluded.

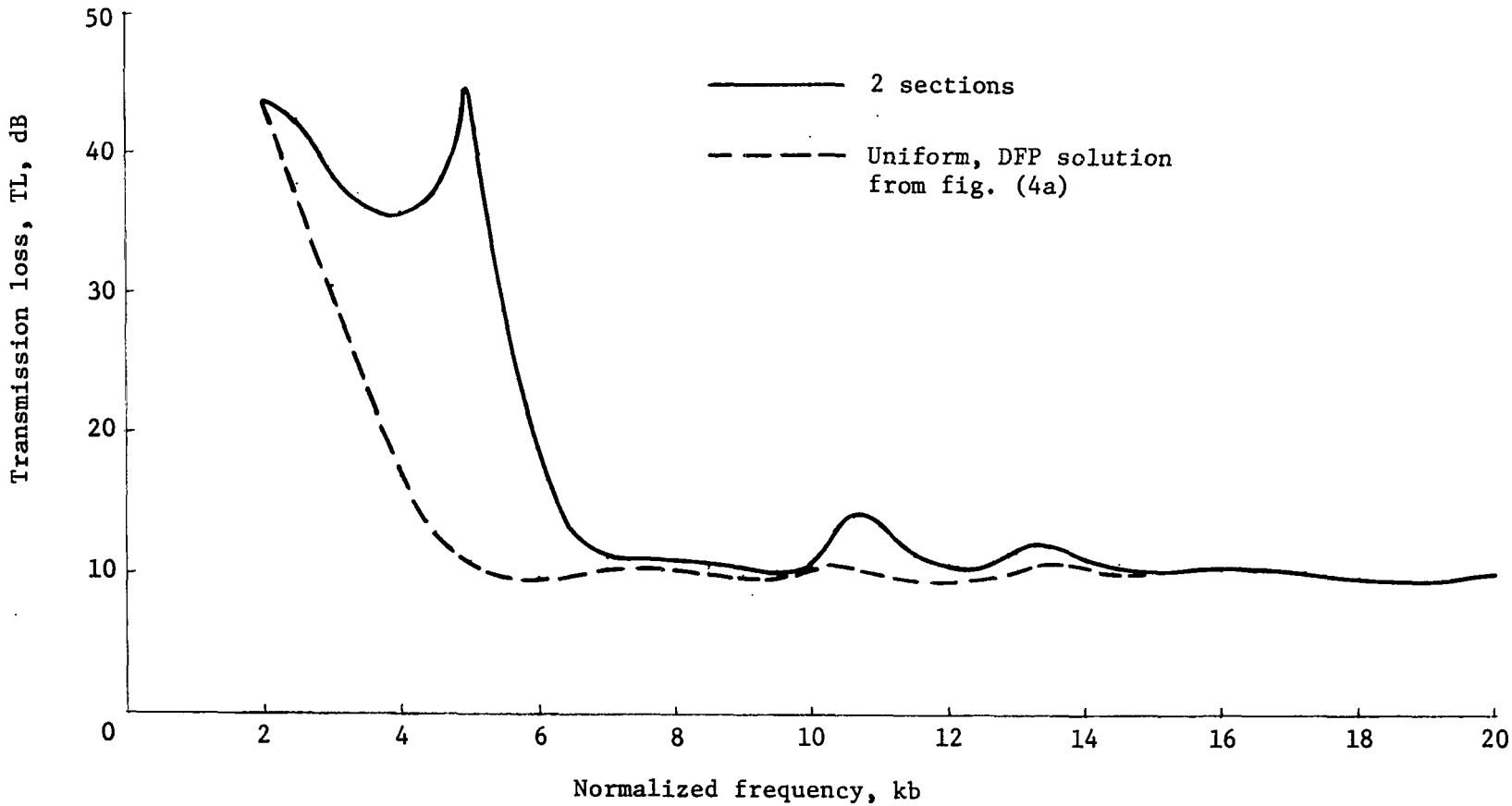

(a) Transmission loss.

Figure 10.- Optimal properties of a two-section circular liner (fig. 8) for a monopole source and L = 2b.

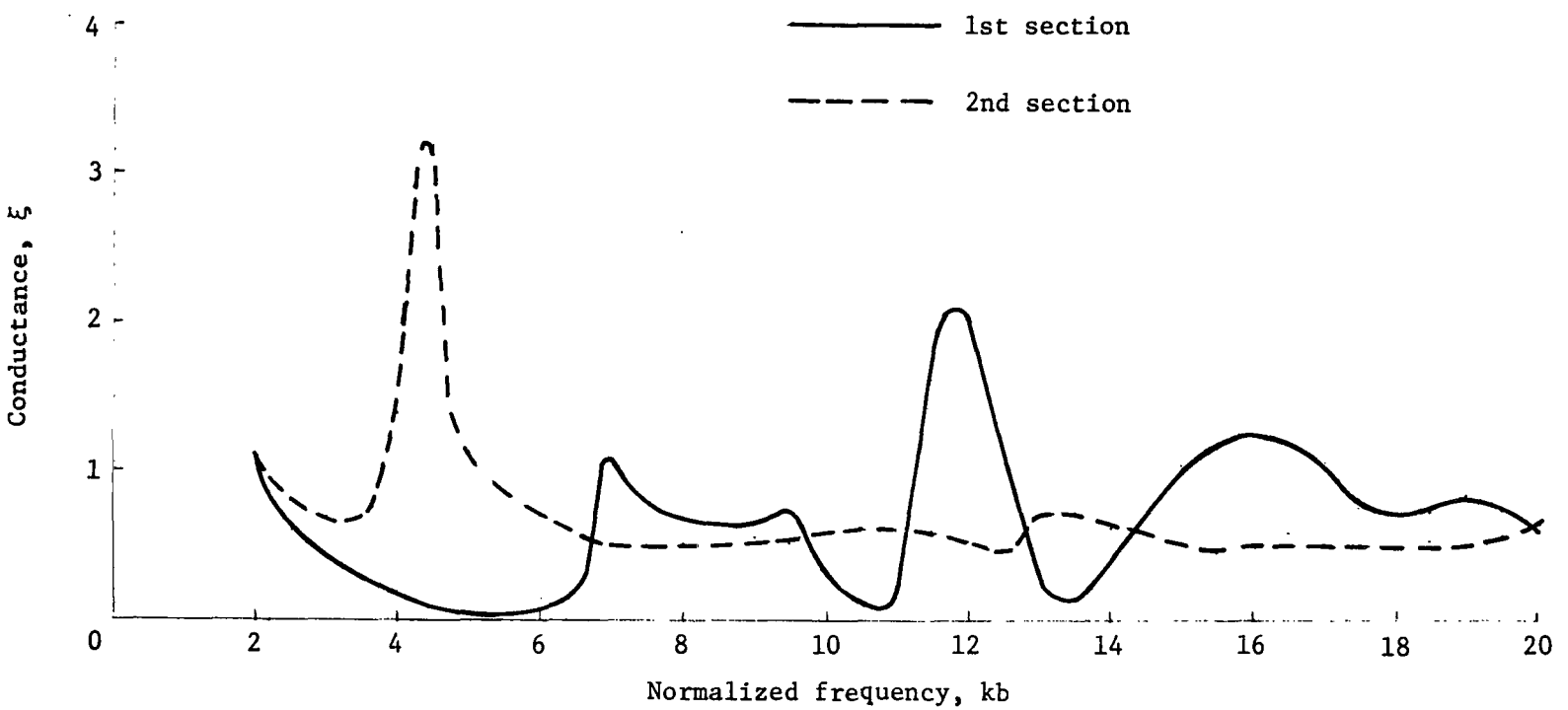

(b) Conductance.

Figure 10.- Continued.

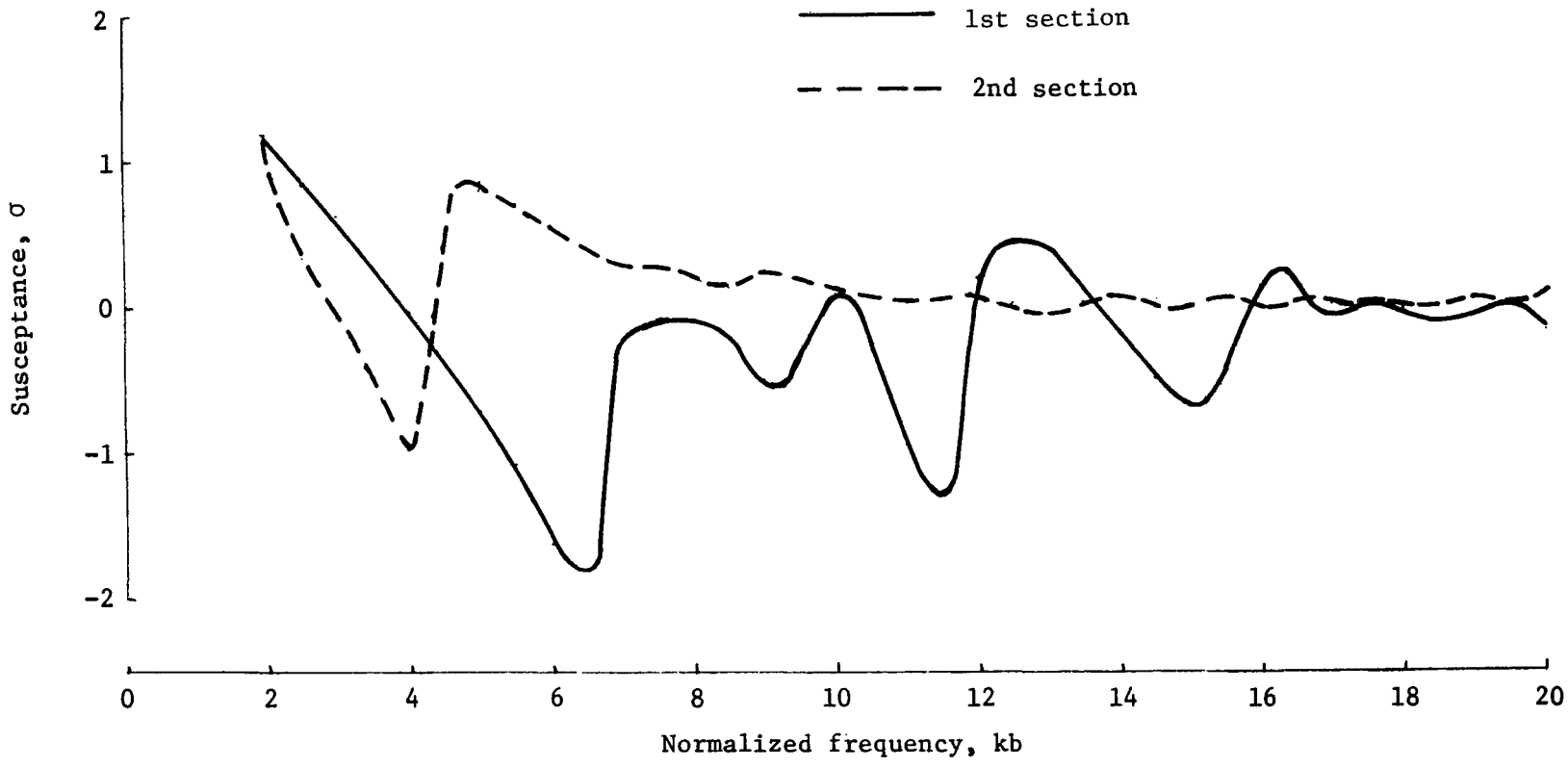

(c) Susceptance.

Figure 10.- Concluded.

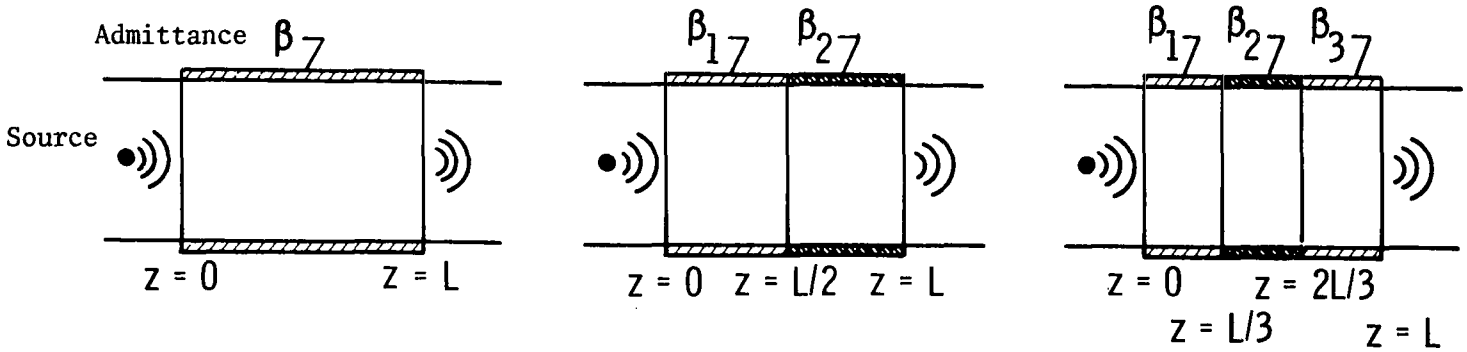

(a) One section. (b) Two sections. (c) Three sections.

Figure 11.- Duct liner configurations for turbomachinery source.

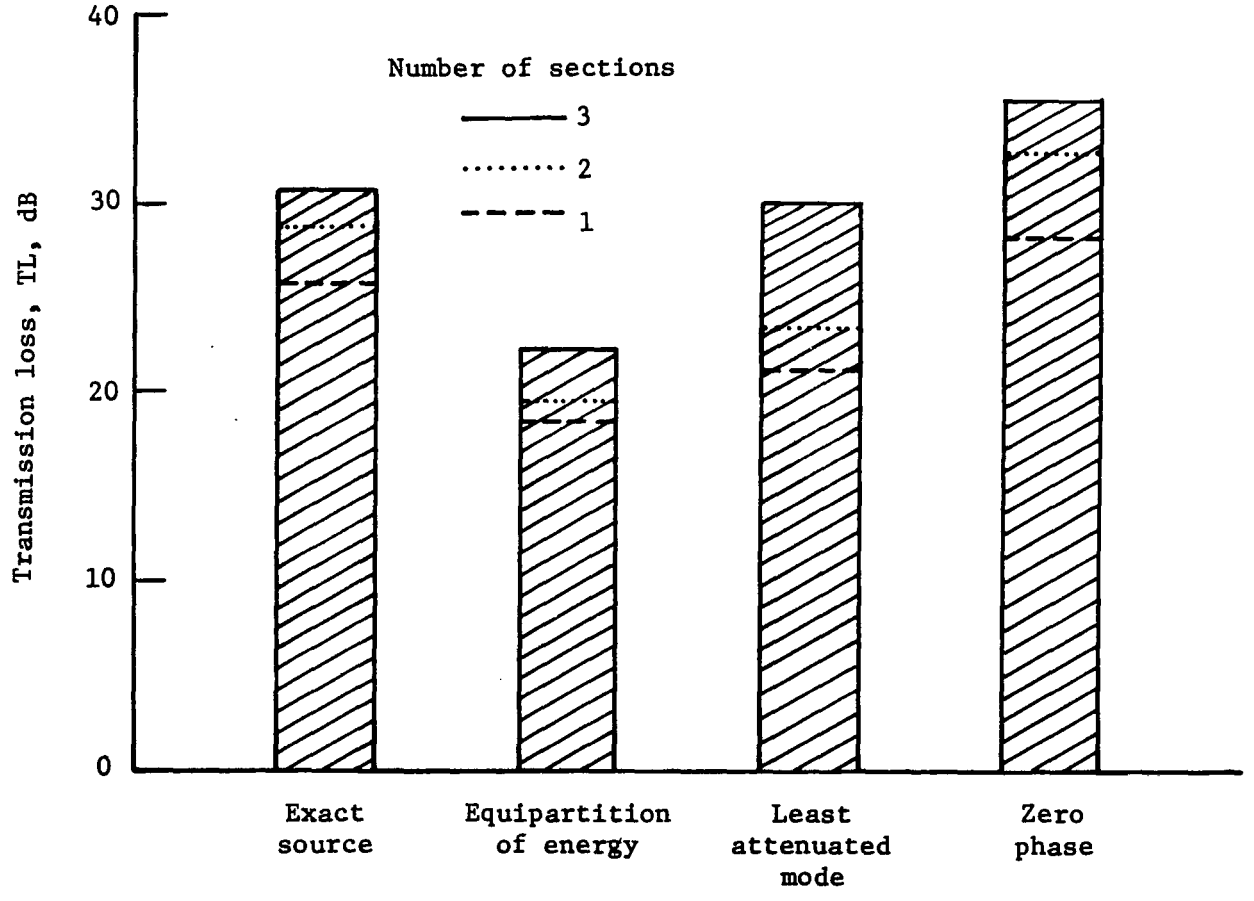

Figure 12.- Maximum transmission loss for a research compressor for different source models. Circular liners (fig. 11); kb = 16.53; Mach number = 0.4; and m = -7.

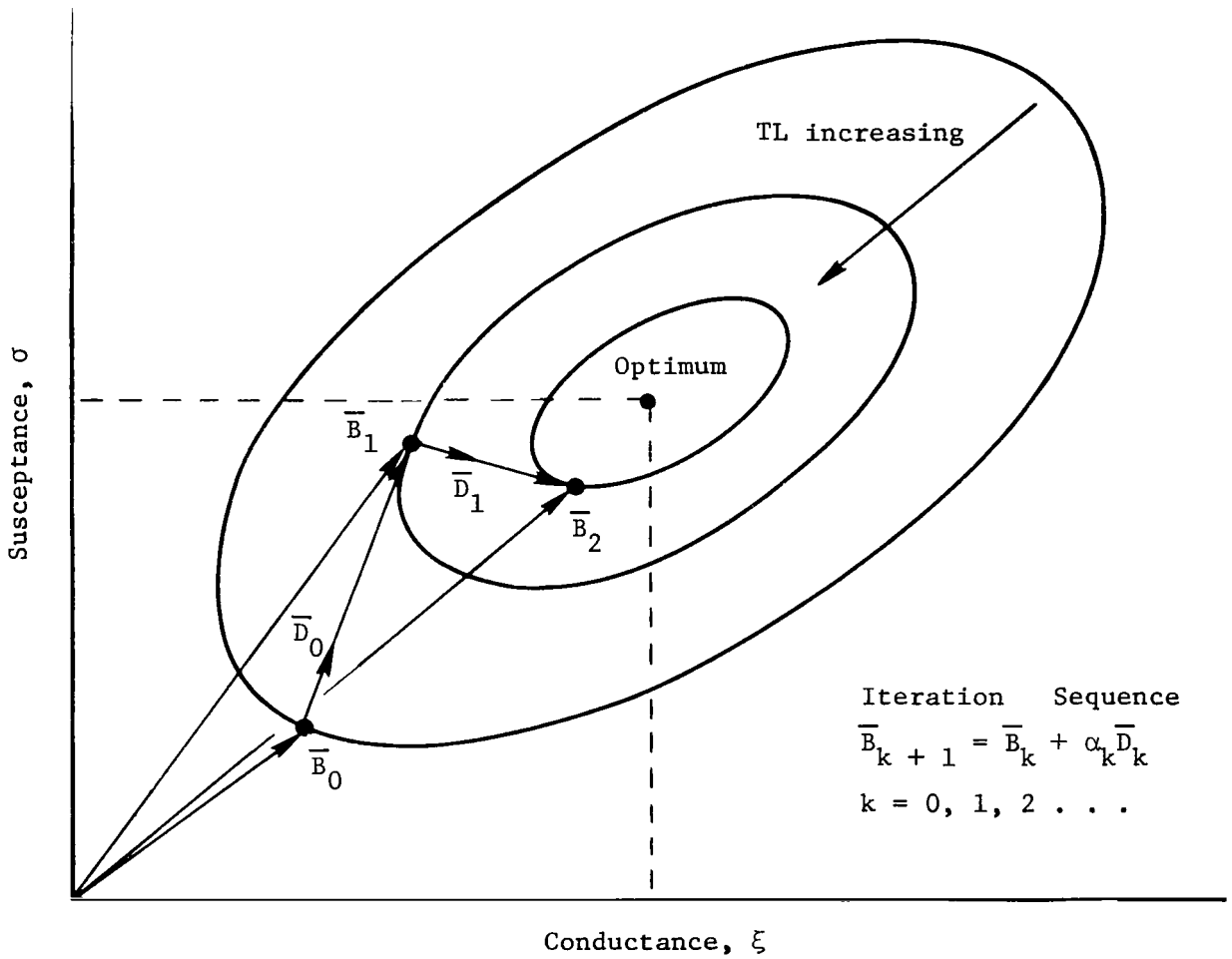

Figure 13.- Optimization strategy.

"The aeronautical and space activities of the United States shall be conducted so as to contribute . . . to the expansion of human knowledge of phenomena in the atmosphere and space. The Administration shall provide for the widest practicable and appropriate dissemination of information concerning its activities and the results thereof."

—NATIONAL AERONAUTICS AND SPACE ACT OF 1958

NASA SCIENTIFIC AND TECHNICAL PUBLICATIONS

TECHNICAL REPORTS: Scientific and technical information considered important, complete, and a lasting contribution to existing knowledge.

TECHNICAL NOTES: Information less broad in scope but nevertheless of importance as a contribution to existing knowledge.

TECHNICAL MEMORANDUMS: Information receiving limited distribution because of preliminary data, security classification, or other reasons. Also includes conference proceedings with either limited or unlimited distribution.

CONTRACTOR REPORTS: Scientific and technical information generated under a NASA contract or grant and considered an important contribution to existing knowledge.

TECHNICAL TRANSLATIONS: Information published in a foreign language considered to merit NASA distribution in English.

SPECIAL PUBLICATIONS: Information derived from or of value to NASA activities. Publications include final reports of major projects, monographs, data compilations, handbooks, sourcebooks, and special bibliographies.

TECHNOLOGY UTILIZATION PUBLICATIONS: Information on technology used by NASA that may be of particular interest in commercial and other non-aerospace applications. Publications include Tech Briefs, Technology Utilization Reports and Technology Surveys.

Details on the availability of these publications may be obtained from:

SCIENTIFIC AND TECHNICAL INFORMATION OFFICE

NATIONAL AERONAUTICS AND SPACE ADMINISTRATION

Washington, D.C. 20546